THE JOURNAL OF PHYSICAL CHEMISTRY A
A JOURNAL OF THE AMERICAN CHEMICAL SOCIETY

pubs.acs.org/JPCA

Article

A Divergence-Free Wigner Transform of the Boltzmann Operator Based on an Effective Frequency Theory

Published as part of The Journal of Physical Chemistry virtual special issue "125 Years of The Journal of Physical Chemistry".

Jens Aage Poulsen and Gunnar Nyman*

Cite This: *J. Phys. Chem. A* 2021, 125, 9209–9225

Read Online

ACCESS | Metrics & More | Article Recommendations | Supporting Information

ABSTRACT: The centroid effective frequency representation of path integrals as developed by Feynman and Kleinert was originally aimed at calculating partition functions and related quantities in the canonical ensemble. In its path integral formulation, only *closed* paths were relevant. This formulation has been used by the present authors in order to calculate the many-body Wigner function of the Boltzmann operator, which includes also open paths. This usage of the theory outside of the original intention can lead to mathematical divergence issues for potentials with barriers, particularly at low temperature. In the present paper, we modify the effective frequency theory of Feynman and Kleinert by also including open paths in its variational equations. In this way, a divergence-free approximation to the Boltzmann operator matrix elements is derived. This generalized version of Feynman and Kleinert's formulation is thus more robust and can be applied to all types of barriers at all temperatures. This new version is used to calculate the Wigner functions of the Boltzmann operator for a quartic oscillator and for a double well potential and both static and dynamic properties are studied at several temperatures. The new theory is found to be essentially as precise as the original one. Its advantage is that it will always deliver a well-defined, even if approximate, Wigner function, which can, for instance, be used for sampling initial conditions for molecular dynamics simulations. As will be discussed, the theory can be systematically improved by including higher-order Fourier modes into the nonquadratic part of the trial action.

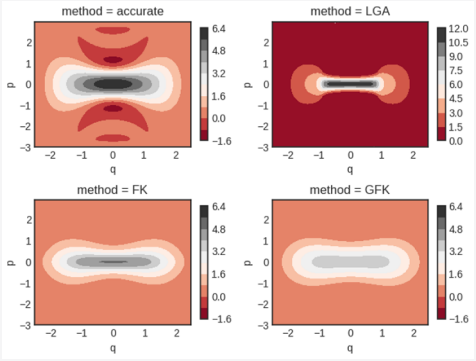

INTRODUCTION

The Wigner transform of the Boltzmann operator, introduced by Wigner almost a century ago,[1] is an important tool for analyzing quantum effects in statistical mechanics; see, e.g., selected papers in ref 2. It has, for instance, served as an inexpensive tool for sampling quantized initial conditions for molecular dynamics simulations; see, e.g., refs 3−6.

Unfortunately, it is only for systems of very limited dimensionality that it is possible to accurately obtain the Wigner transform of the Boltzmann operator. Due to its usefulness, the Wigner transform and the problem of its computation is, however, the subject of intense ongoing research.[6−11] Consequently, many approximate schemes for computing the Boltzmann Wigner transform also of large systems have now been put forth.[3,5,6,12−16] Many of these methods rely on introducing various harmonic approximations in the otherwise intractable mathematical expressions.[3−6,12] This enables a sufficient simplification of the equations so that an approximate, multidimensional Wigner transform can be computed.

The harmonic models sadly show a serious shortcoming when they are applied to problems involving potential barriers in that the Wigner transform diverges at low temperature and/or large potential curvature.[3−5,12] More specifically, it is the off-diagonal part of the density operator matrix elements

$$\langle q - \frac{\eta}{2}|\hat{\rho}|q + \frac{\eta}{2}\rangle \tag{1}$$

that becomes meaningless when $\hbar|\Omega|\beta > \pi$. Here q is a coordinate, η is the off-diagonal distance, $\hat{\rho}$ is the density operator, Ω is the imaginary frequency, and $\beta = 1/(k_B T)$ where T is the absolute temperature. Under such conditions this matrix element essentially becomes $\exp(-\alpha\eta^2)$ with $\alpha < 0$; see, e.g., refs 3 and 12.

The momentum part of the Wigner transform is the Fourier transform of the off-diagonal part of the density operator. From the previous paragraph it can be seen that it becomes ill-

Received: July 1, 2021
Revised: September 23, 2021
Published: October 12, 2021

https://doi.org/10.1021/acs.jpca.1c05860
J. Phys. Chem. A 2021, 125, 9209−9225

defined when $\hbar|\Omega|\beta > \pi$. Although all *moments* of p can still be calculated even when $\alpha < 0$, the Wigner function cannot be used for *sampling* momenta. This is a serious limitation of the harmonic models and ways to modify them have been proposed. For example, Liu and Miller[12] put forth an ad-hoc extrapolation of the Gaussian momentum exponent α into the forbidden regime, so that a well-defined sampling function exists for all temperatures and frequencies. Poulsen and co-workers have simply chosen to set the momenta to zero and skip the sampling when $\hbar|\Omega|\beta > \pi$, which is a continuous extrapolation of the $\hbar|\Omega|\beta \leq \pi$ case; see, e.g., refs 3, 15, and 17.

The harmonic scheme of Poulsen et al.[3,15] for calculating Wigner transforms is an adoption of the effective frequency theory of Feynman and Kleinert.[18,19] This scheme has been applied quite successfully to a number of problems in condensed phase involving the quantization of several hundred degrees of freedom. More specifically, the method has been used for calculating dynamic structure factors[15,20−22] and diffusion coefficients in liquids.[17,23,24] Despite its relative success, this scheme may be considered as an *illegitimate* extension of the effective frequency theory of Feynman and Kleinert in the sense that the latter is a theory for approximating path integrals involving only *closed* paths, while Poulsen et al.[3] nevertheless applied it to path integrals which include open paths as well.

Strictly speaking, the extension discussed above is uncontrollable, meaning that divergence problems show up since the effective frequencies are not optimized for open paths. As already explained, these problems appear for barrier potentials at low temperature and this is the reason why the theory has not been applied to reaction rate problems, where a so-called thermalized flux Wigner distributions must be computed.[12] Reaction rate theory is a central subject in chemistry and it is therefore highly desirable to solve this problem.

The subject of the present paper is to fix the barrier problem by developing an effective frequency theory tailored to path integrals also involving *open* paths. It will be the first rigorous effective frequency model which can calculate off-diagonal elements of the Boltzmann operator and can be combined with general potentials at all temperatures. The theory derived here may be regarded as a first step toward making the effective frequency theory applicable also to reaction rate problems. The derivation is relatively similar to the original one by Feynman and Kleinert;[18,19] the main difference is the inclusion of open paths, which makes the mathematics slightly more involved.

This paper is structured such that after the above "Introduction" there is a long section on "Methods" where we, based on the Feynman−Kleinert (FK) closed path approach, derive new iterative equations by generalizing the FK approach to include also open paths. This gives us the *Generalized Feynman−Kleinert* (GFK) approach. Thereafter follows a "Results" section before we end with "Discussion and Conclusions".

METHODS

For simplicity, we formulate the GFK theory in one dimension. The new theory is generalized to several dimensions in the same way as the original Feynman−Kleinert theory; see ref 3. In what follows we, for simplicity, frequently refer to open paths but then actually meaning both open and closed paths unless it is clear from the context that we only consider open paths. We will consider a particle with mass M moving in the potential $V(x)$ at an inverse temperature $\beta = 1/k_B T$.

The open path effective frequency theory is derived by first considering the Feynman path integral for the Boltzmann operator:

$$\exp(-\beta\hat{H}) = \int \mathrm{d}x\ \mathrm{d}x' \int_{x(0)=x}^{x(\beta\hbar)=x'} |x'\rangle\langle x|\ \mathrm{D}x(\tau)\ \exp(-S[x(\tau)]/\hbar) \tag{2}$$

with

$$S[x(\tau)] = \int_0^{\beta\hbar} \mathrm{d}\tau \left\{ \frac{M}{2}\dot{x}(\tau)^2 + V(x(\tau)) \right\} \tag{3}$$

The centroid of a path, x_c, is the average value of the path:

$$x_c = \frac{1}{\beta\hbar}\int_0^{\beta\hbar} \mathrm{d}\tau\ x(\tau) \tag{4}$$

We next express the Boltzmann operator using localized operators, $\hat{\Delta}(x_c)$, whose path integral representations are each restricted to paths with a certain centroid. We write

$$\exp(-\beta\hat{H}) = \int \mathrm{d}x_c\ \hat{\Delta}(x_c) \tag{5}$$

where

$$\hat{\Delta}(x_c) = \int \mathrm{d}x\ \mathrm{d}x' \int_{x(0)=x}^{x(\beta\hbar)=x'} |x'\rangle\langle x|\ \mathrm{D}x(\tau)\ \delta(\bar{x} - x_c)\ \exp(-S[x(\tau)]/\hbar) \tag{6}$$

We now introduce a new quantity, the *off-diagonal* trace as

$$\Delta(x_c) = \int \mathrm{d}x\ \mathrm{d}x' \int_{x(0)=x}^{x(\beta\hbar)=x'} \mathrm{D}x(\tau)\ \delta(\bar{x} - x_c)\ \exp(-S[x(\tau)]/\hbar) \tag{7}$$

which differs from a standard trace by also including open paths. Due to the delta-function, it is unitless.[a] In the following we will use the short-hand notation

$$\Delta(x_c) = \int \mathrm{D}x(\tau)\ \delta(\bar{x} - x_c)\ \exp(-S[x(\tau)]/\hbar) \tag{8}$$

instead of eq 7. There is no ambiguity in this expression since we consider both closed and open paths. *Thus, in the following* $\int \mathrm{D}x(\tau)$ *always means integration over closed and open paths.* The idea is now to exploit the introduced locality when calculating the above quantities.

In the high temperature limit, $\hat{\Delta}(x_c)$ is dominated by paths that only probe a small neighborhood around their centroids. This suggests substituting the actual potential in eq 3 by a *trial* potential of the form

$$V_{\Omega(x_c),L(x_c)}(x(\tau)) = L(x_c) + \frac{1}{2}M\Omega^2(x_c)(x(\tau) - x_c)^2 \tag{9}$$

which is of the same form as used by Feynman and Kleinert. Such a potential should work extremely well at high temperatures. The same form will, however, be used for all temperatures.

For each centroid, two unknown parameters $L(x_c)$ and $\Omega^2(x_c)$ must be determined. As we shall see, their values can respectively be thought of as representing a smeared potential and its second derivative similarly smeared and both evaluated

https://doi.org/10.1021/acs.jpca.1c05860
J. Phys. Chem. A 2021, 125, 9209−9225

around x_c. The smearing width will be derived from the "size" of all paths (open and closed) associated with that centroid.

Once $L(x_c)$ and $\Omega^2(x_c)$ have been found, we can integrate out *all* path variables in eq 6 except the centroid; see below. This makes the effective frequency theory powerful: the original multidimensional path integral becomes one-dimensional and the Wigner transform can be calculated (see eq 48 in ref 3). Thus, as shown in Appendix A, the Wigner transform of $\hat{\Delta}(x_c)$ becomes

$$(\hat{\Delta}_{tr}(x_c))_W[q,p] = \exp(-\beta L(x_c))\frac{\frac{\hbar}{2}\beta\Omega(x_c)}{\sinh\left(\frac{\hbar}{2}\beta\Omega(x_c)\right)}\left(\frac{\tanh\left(\frac{\hbar}{2}\beta\Omega(x_c)\right)}{a_{FK}{}^2(x_c)\pi\Omega(x_c)\hbar\beta}\right)^{1/2} \times \exp\left(-\frac{1}{2a_{FK}{}^2(x_c)}(q-x_c)^2 - \frac{\tanh\left(\frac{\hbar}{2}\beta\Omega(x_c)\right)}{M\Omega(x_c)\hbar}p^2\right) \tag{10}$$

where *tr* stands for trial and $a_{FK}{}^2(x_c)$ is given by

$$a_{FK}{}^2(x_c) = \frac{1}{M\Omega^2(x_c)\beta}\left\{\frac{\hbar\Omega(x_c)\beta}{2}\coth\left(\frac{\hbar\Omega(x_c)\beta}{2}\right) - 1\right\} \tag{11}$$

$a_{FK}{}^2(x_c)$ comes from Feynman and Kleinert's original theory and has dimensions length squared. For imaginary $\Omega(x_c)$ the exponent in the momentum part contains $\tan\left(\frac{\hbar}{2}\beta|\Omega(x_c)|\right)$ which diverges when $\hbar|\Omega(x_c)|\beta = \pi$; see ref 3. We point out that eq 10 is the same in the original FK theory and the new generalized effective frequency theory presented here (GFK). The values of $\Omega(x_c)$ and $L(x_c)$ as functions of x_c on the other hand differ between the two theories.

Let us now determine $L(x_c)$ and $\Omega^2(x_c)$ for a given centroid x_c. The task is to replace $V(x(\tau))$ in $\hat{\Delta}(x_c)$ or $\Delta(x_c)$ with $L(x_c) + \frac{1}{2}M\Omega^2(x_c)(x(\tau)-x_c)^2$ in the best possible way. After replacement, the off-diagonal trace $\Delta(x_c)$ is transformed into $\Delta_{tr}(x_c)$, where

$$\Delta_{tr}(x_c) = \int \mathrm{D}x\,(\tau)\delta(\bar{x}-x_c)\exp(-S_{tr}^{x_c}[x(\tau)]/\hbar) \tag{12}$$

$$S_{tr}^{x_c}[x(\tau)] = \int_0^{\beta\hbar}\mathrm{d}\tau\left\{\frac{M}{2}\dot{x}(\tau)^2 + L(x_c) + \frac{1}{2}M\Omega^2(x_c)(x(\tau)-x_c)^2\right\} \tag{13}$$

The off-diagonal trace corresponding to the full Boltzmann operator is approximated as

$$\int \mathrm{d}x_c\,\Delta(x_c) \approx \int \mathrm{d}x_c\,\Delta_{tr}(x_c) = \tag{14}$$

$$\int \mathrm{d}x_c \int \mathrm{D}x(\tau)\,\delta(\bar{x}-x_c)\exp(-S_{tr}^{x_c}[x(\tau)]/\hbar) = \int \mathrm{D}x(\tau)\exp(-S_{tr}^{x_c}[x(\tau)]/\hbar) \tag{15}$$

where we notice that the last equality above is perfectly meaningful since the value of x_c in $S_{tr}^{x_c}[x(\tau)]$ is determined by x_c in the path integration $\int \mathrm{D}x(\tau)$.

In order to make $\int \mathrm{d}x_c\,\Delta_{tr}(x_c)$ be as close as possible to $\int \mathrm{d}x_c\,\Delta(x_c)$ we use the Jensen inequality.[25] We start by writing the exact path integral as

$$\int \mathrm{d}x_c\,\Delta(x_c) = \int \mathrm{D}x(\tau)\exp(-S[x(\tau)]/\hbar) = \int \mathrm{d}x_c\,\Delta_{tr}(x_c) \times \frac{\int \mathrm{D}x(\tau)\exp(-\{S[x(\tau)] - S_{tr}^{x_c}[x(\tau)]\}/\hbar)\times\exp(-S_{tr}^{x_c}[x(\tau)]/\hbar)}{\int \mathrm{d}x_c\,\Delta_{tr}(x_c)} \tag{16}$$

or

$$\int \mathrm{d}x_c\,\Delta(x_c) = \int \mathrm{d}x_c\,\Delta_{tr}(x_c) \times \langle\exp(-\{S[x(\tau)] - S_{tr}^{x_c}[x(\tau)]\}/\hbar)\rangle_{tr} \tag{17}$$

where the average of a function f is calculated by

$$\langle f[x(\tau)]\rangle_{tr} = \frac{\int \mathrm{D}x(\tau)\,f[x(\tau)]\times\exp(-S_{tr}^{x_c}[x(\tau)]/\hbar)}{\int \mathrm{d}x_c\,\Delta_{tr}(x_c)} \tag{18}$$

The Jensen inequality[25] rests on the convexity of the exponential function and states that

$$\lambda_1\exp(\varphi_1) + \lambda_2\exp(\varphi_2) \geq \exp(\lambda_1\varphi_1 + \lambda_2\varphi_2), \quad \lambda_1 + \lambda_2 = 1 \tag{19}$$

where φ_1 and φ_2 are arbitrary real numbers. Its integral variant is[25]

$$\int \mathrm{d}x\,\lambda(x)\exp(\varphi(x)) \geq \exp\left(\int \mathrm{d}x\,\lambda(x)\,\varphi(x)\right), \quad \int \mathrm{d}x\,\lambda(x) = 1 \tag{20}$$

Using eq 20 in its multidimensional version with $\lambda[x(\tau)] = \exp(-S_{tr}^{x_c}[x(\tau)]/\hbar)/\int \mathrm{d}x_c\,\Delta_{tr}(x_c)$, so that $\int \mathrm{D}x(\tau)\,\lambda[x(\tau)] = 1$, and $\varphi[x(\tau)] = -(S[x(\tau)] - S_{tr}^{x_c}[x(\tau)])/\hbar$, we obtain

$$\int \mathrm{d}x_c\,\Delta(x_c) \geq \int \mathrm{d}x_c\,\Delta_{tr}(x_c) \times \exp(-\langle[S[x(\tau)] - S_{tr}^{x_c}[x(\tau)]\rangle_{tr}/\hbar) \tag{21}$$

We will thus seek the values of $L(x_c)$ and $\Omega^2(x_c)$ that maximize the right-hand side of eq 21. For this purpose we derive an expression for $\Delta_{tr}(x_c)$ in Appendix A using results from ref 3 and obtain

$$\Delta_{tr}(x_c) = \exp(-\beta L(x_c))\frac{\frac{\hbar}{2}\beta\Omega(x_c)}{\sinh\left(\frac{\hbar}{2}\beta\Omega(x_c)\right)}\left(\frac{\tanh\left(\frac{\hbar}{2}\beta\Omega(x_c)\right)}{\frac{\hbar}{2}\Omega(x_c)\beta}\right)^{1/2} = \exp(-\beta L(x_c))\left(\frac{\hbar\Omega(x_c)\beta}{\sinh(\hbar\beta\Omega(x_c))}\right)^{1/2} \equiv \alpha(x_c)\exp(-\beta L(x_c)) \tag{22}$$

Next we wish to evaluate

https://doi.org/10.1021/acs.jpca.1c05860
J. Phys. Chem. A 2021, 125, 9209−9225

$$\langle S[x(\tau)] - S_{tr}^{x_c}[x(\tau)]\rangle_{tr} = \frac{\int dx_c \int \mathrm{D}x(\tau)\, \delta(\bar{x} - x_c) \times \int_0^{\beta\hbar} d\tau \left(V(x(\tau)) - L(x_c) - \frac{1}{2}M\Omega^2(x_c)(x(\tau) - x_c)^2\right) \times \exp(-S_{tr}^{x_c}[x(\tau)]/\hbar)}{\int dx_c\, \Delta_{tr}(x_c)}$$
$$= \frac{\int dx_c\, \Delta_{tr}(x_c) \times \frac{\int \mathrm{D}x\,(\tau)\delta(\bar{x} - x_c)}{\Delta_{tr}(x_c)} \int_0^{\beta\hbar} d\tau \left(V(x(\tau)) - L(x_c) - \frac{1}{2}M\Omega^2(x_c)(x(\tau) - x_c)^2\right) \times \exp(-S_{tr}^{x_c}[x(\tau)]/\hbar)}{\int dx_c\, \Delta_{tr}(x_c)} \tag{23}$$

The quantity

$$\langle S[x(\tau)] - S_{tr}[x(\tau)]\rangle_{tr} x_c \equiv \frac{\int \mathrm{D}x(\tau)\, \delta(\bar{x} - x_c)}{\Delta_{tr}(x_c)} \int_0^{\beta\hbar} d\tau \left(V(x(\tau)) - L(x_c) - \frac{1}{2}M\Omega^2(x_c)(x(\tau) - x_c)^2\right) \times \exp(-S_{tr}^{x_c}[x(\tau)]/\hbar) \tag{24}$$

appearing in eq 23 is also an expectation value, using again the weight-function $\exp(-S_{tr}^{x_c}[x(\tau)]/\hbar)$ but now evaluated for a *fixed* centroid x_c as opposed to in eq 18 where x_c is integrated over.

We may write

$$\langle S[x(\tau)] - S_{tr}[x(\tau)]\rangle_{tr}^{x_c} = \int_0^{\beta\hbar} d\tau \left\{ \langle V(x(\tau))\rangle_{tr}^{x_c} - L(x_c) - \frac{1}{2}M\Omega^2(x_c)\langle (x(\tau) - x_c)^2)\rangle_{tr}^{x_c} \right\} \tag{25}$$

where we need to calculate the different terms. Let us first look at the average square position found in the last term:

$$\langle x^2(\tau)\rangle_{tr}^{x_c} = \int \mathrm{D}x(\tau)\, \delta(\bar{x} - x_c) \times x^2(\tau) \times \exp(-S_{tr}^{x_c}[x(\tau)]/\hbar)/\Delta_{tr}(x_c) \tag{26}$$

To evaluate this, we write the paths explicitly using their Fourier representation. As will be seen, once this special term has been found, all other quantities follow straightforwardly. The paths in eq 26 include all closed and open paths $x(\tau)$ with a common centroid x_c.

We wish to find a Fourier representation suitable for describing open paths where x_c occurs explicitly as a Fourier mode. We also need to evaluate the time derivative of $x(\tau)$ so that we can calculate the kinetic energy of the path. This means that we need to interchange the infinite summation and differentiation operations in our Fourier series expression. This is permissible if $x(\tau)$ is continuous and $x'(\tau)$ is integrable.[26] Thus, we cannot adopt the Fourier series of $x(\tau)$ directly by regarding it as a $\beta\hbar$-periodic function, since this function is discontinuous at its open ends. We can instead achieve our requirements by considering a *continuous extension* of $x(\tau)$ as follows.

We extend our open paths to new ones, $\tilde{x}(\tau)$, defined on the double time interval $0 < \tau < 2\beta\hbar$. We shall require that our extended paths be identical to the old ones in the original time window: $\tilde{x}(\tau) = x(\tau)$, $0 < \tau < \beta\hbar$ and further that they are symmetric around $\tau = \beta\hbar$, i.e., $\tilde{x}(\tau) = \tilde{x}(2\beta\hbar - \tau)$, which fully determines $\tilde{x}(\tau)$. By this prescription there is a one-to-one correspondence between the $x(\tau)$ and $\tilde{x}(\tau)$ paths. Further, due to the symmetry, the centroids of $x(\tau)$ and $\tilde{x}(\tau)$ are identical.

The $\tilde{x}(\tau)$ paths can be defined for all real τ by letting $\tilde{x}(\tau)$ be $2\beta\hbar$-periodic. The $\tilde{x}(\tau)$ paths are closed paths, and if we restrict them to be physical, continuous paths, they fulfill all our requirements. We may then write the Fourier series

$$\tilde{x}(\tau) = a_0 + \sum_{n=1}^{\infty} a_n \cos\left(\frac{2\pi n\tau}{2\beta\hbar}\right) + b_n \sin\left(\frac{2\pi n\tau}{2\beta\hbar}\right) = a_0 + \sum_{n=1}^{\infty} a_n \cos\left(\frac{\pi n\tau}{\beta\hbar}\right) + b_n \sin\left(\frac{\pi n\tau}{\beta\hbar}\right) \tag{27}$$

where $b_n = 0$ for all n, due to the reflection property of $\tilde{x}(\tau)$ around $\tau = \beta\hbar$. If we restrict this Fourier series to $0 < \tau < \beta\hbar$, we obtain our desired open path representation

$$x(\tau) = a_0 + \sum_{n=1}^{\infty} a_n \cos\left(\frac{\pi n\tau}{\beta\hbar}\right), \qquad 0 < \tau < \beta\hbar \tag{28}$$

The basis functions are orthogonal:

$$\int_0^{\beta\hbar} d\tau \cos\left(\frac{\pi m\tau}{\beta\hbar}\right) \cos\left(\frac{\pi n\tau}{\beta\hbar}\right) = \frac{1}{2}\delta_{mn} \times \beta\hbar \tag{29}$$

Clearly, a_0 is the common centroid of $x(\tau)$ and $\tilde{x}(\tau)$:

$$a_0 = \frac{1}{\beta\hbar}\int_0^{\beta\hbar} d\tau\, x(\tau) = \frac{1}{2\beta\hbar}\int_0^{2\beta\hbar} d\tau\, \tilde{x}(\tau) \tag{30}$$

Likewise, it follows from eq 28 that

$$a_n = \frac{2}{\beta\hbar}\int_0^{\beta\hbar} d\tau\, x(\tau) \cos\left(\frac{\pi n\tau}{\beta\hbar}\right) \tag{31}$$

In Appendix B, we derive eq 28 again but by using the normal modes of the open polymer. We also show how to set up a general path integral using the path parametrization in eq 28. If we write $\omega_n = \frac{\pi n}{\beta\hbar}$, the trial action can now be evaluated as ($x_c = a_0$)

$$S_{tr}^{x_c}[x(\tau)] = \int_0^{\beta\hbar} d\tau \left\{ \frac{M}{2}\dot{x}(\tau)^2 + L(x_c) + \frac{1}{2}M\Omega^2(x_c)(x(\tau) - x_c)^2 \right\} = \frac{M\beta\hbar}{2} \sum_{n=1}^{\infty} [\omega_n{}^2 + \Omega^2(x_c)]\frac{a_n{}^2}{2} + \beta\hbar L(x_c) \tag{32}$$

Returning now to eq 26, we write[b]

https://doi.org/10.1021/acs.jpca.1c05860
J. Phys. Chem. A 2021, 125, 9209−9225

$$\langle x^2(\tau)\rangle_{tr}^{x_c} = \int \mathrm{D}x(\tau)\,\delta(\bar{x} - x_c) \times x^2(\tau) \times \exp(-S_{tr}^{x_c}[x(\tau)]/\hbar)/\Delta_{tr}(x_c)$$
$$= \frac{\int\prod_{n=1}^{\infty} \mathrm{d}a_n\, x^2(\tau)\exp\left(-\beta\frac{M}{2}\sum_{n=1}^{\infty}[\omega_n^2 + \Omega^2(x_c)]\frac{a_n^2}{2} - \beta L(x_c)\right)}{\int\prod_{n=1}^{\infty} \mathrm{d}a_n \exp\left(-\beta\frac{M}{2}\sum_{n=1}^{\infty}[\omega_n^2 + \Omega^2(x_c)]\frac{a_n^2}{2} - \beta L(x_c)\right)}$$
$$= \frac{\int\prod_{n=1}^{\infty} \mathrm{d}a_n\,[x_c + \sum_{n=1}^{\infty} a_n\cos(\omega_n\tau)]^2\exp\left(-\beta\frac{M}{2}\sum_{n=1}^{\infty}[\omega_n^2 + \Omega^2(x_c)]\frac{a_n^2}{2}\right)}{\int\prod_{n=1}^{\infty} \mathrm{d}a_n \exp\left(-\beta\frac{M}{2}\sum_{n=1}^{\infty}[\omega_n^2 + \Omega^2(x_c)]\frac{a_n^2}{2}\right)}$$
$$= x_c^2 + \frac{2}{M\beta}\sum_{n=1}^{\infty}\frac{\cos^2(\omega_n\tau)}{\omega_n^2 + \Omega^2(x_c)} = x_c^2 + \frac{1}{M\beta}\sum_{n=1}^{\infty}\frac{1 + \cos(2\omega_n\tau)}{\omega_n^2 + \Omega^2(x_c)} \tag{33}$$

Using the result (see page 83 in ref 27)

$$\frac{1}{2a^2} + \sum_{n=1}^{\infty}\frac{\cos(n\theta)}{n^2 + a^2} = \frac{\pi}{2a}\frac{\cosh((\pi - |\theta|)a)}{\sinh(\pi a)} \tag{34}$$

it is shown in Appendix A that

$$\langle x^2(\tau)\rangle_{tr}^{x_c} = x_c^2 + a_{FK}^2(x_c) + \frac{\hbar}{M\Omega(x_c)}\frac{\sinh^2(\Omega(x_c)(\beta\hbar/2 - \tau))}{\sinh(\Omega(x_c)\beta\hbar)} \tag{35}$$

Here the smearing width $a_{FK}^2(x_c)$, given in eq 11, has appeared. In the closed path theory we would find the simpler result: $\langle x^2(\tau)\rangle_{tr}^{x_c} = x_c^2 + a_{FK}^2(x_c)$. Naturally, for closed paths, the quantum fluctuations are independent of τ. According to eq 35, however, for open paths, fluctuations are smallest for intermediate times $\tau \sim \beta\hbar/2$ where $\langle x^2(\tau)\rangle_{tr}^{x_c} \sim x_c^2 + a_{FK}^2(x_c)$, while they increase exponentially as $\tau \to 0, \beta\hbar$.

Since both the second and third terms in eq 35 vanish for high temperatures, it seems reasonable to define a new time-dependent *open-path* smearing width as

$$a^2(x_c, \tau) = a_{FK}^2(x_c) + \frac{\hbar}{M\Omega(x_c)}\frac{\sinh^2(\Omega(x_c)(\beta\hbar/2 - \tau))}{\sinh(\Omega(x_c)\beta\hbar)} \tag{36}$$

The last term in this quantity diverges for imaginary $\Omega(x_c)$ when $|\Omega(x_c)|\beta\hbar = \pi$ and becomes infinite when $|\Omega(x_c)|\beta\hbar \to \pi$ from below. The old smearing width $a_{FK}^2(x_c)$ on the other hand does not diverge until $|\Omega(x_c)|\beta\hbar = 2\pi$. Here we find the reason as to why the new theory is well-behaved and the old not. As $|\Omega(x_c)|\beta\hbar \to \pi$ from below, the momentum sampling should start to get problematic, but it does not because *at the same time* $a^2(x_c, \tau)$ goes to infinity thereby making $|\Omega(x_c)|$ smaller in size, since the latter is the Hessian of the potential averaged over $a^2(x_c, \tau)$; see below. The reduced size of $|\Omega(x_c)|$ pushes $|\Omega(x_c)|\beta\hbar$ away from π.

Returning to eq 25, we see that we need to find

$$\int_0^{\beta\hbar}\mathrm{d}\tau\,\langle(x(\tau) - x_c)^2)\rangle_{tr}^{x_c} = \int_0^{\beta\hbar}\mathrm{d}\tau\,\langle x(\tau)^2\rangle_{tr}^{x_c} - \beta\hbar x_c^2 \tag{37}$$

Inserting eq 35 in eq 37 and integrating over τ, we obtain

$$\int_0^{\beta\hbar}\mathrm{d}\tau\,\langle(x(\tau) - x_c)^2)\rangle_{tr}^{x_c} = \beta\hbar a_{FK}^2(x_c) + \hbar\frac{\sinh(\beta\hbar\Omega(x_c)) - \beta\hbar\Omega(x_c)}{2M\Omega^2(x_c)\sinh(\hbar\Omega(x_c)\beta)} \tag{38}$$

The average smearing width over the whole open path thus becomes

$$a^2(x_c) = \frac{1}{\beta\hbar}\int_0^{\beta\hbar}\mathrm{d}\tau\,\langle(x(\tau) - x_c)^2)\rangle_{tr}^{x_c} = a_{FK}^2(x_c) + \frac{\sinh(\beta\hbar\Omega(x_c)) - \beta\hbar\Omega(x_c)}{2\beta M\Omega^2(x_c)\sinh(\hbar\Omega(x_c)\beta)} \tag{39}$$

We now turn our attention to the term $\langle V(x(\tau))\rangle_{tr}^{x_c}$ in eq 25. An easy way to find it is to consider the Fourier representation of the potential:

$$V(x(\tau)) = \frac{1}{2\pi}\int_{-\infty}^{\infty}\mathrm{d}k\,\tilde{V}(k)\exp(\mathrm{i}kx(\tau)) \tag{40}$$

Using eq 28, we obtain

$$\langle V(x(\tau))\rangle_{tr}x_c = \frac{1}{2\pi}\int_{-\infty}^{\infty}\mathrm{d}k\,\tilde{V}(k) \times \frac{\int\prod_{n=1}^{\infty}\mathrm{d}a_n\exp(\mathrm{i}ka_0 + \mathrm{i}k\sum_{n=1}^{\infty}a_n\cos(\omega_n\tau))\exp\left(-\beta\frac{M}{2}\sum_{n=1}^{\infty}[\omega_n^2 + \Omega^2(x_c)]\frac{a_n^2}{2}\right)}{\int\prod_{n=1}^{\infty}\mathrm{d}a_n\exp\left(-\beta\frac{M}{2}\sum_{n=1}^{\infty}[\omega_n^2 + \Omega^2(x_c)]\frac{a_n^2}{2}\right)}$$
$$= \frac{1}{2\pi}\int_{-\infty}^{\infty}\mathrm{d}k\,\tilde{V}(k)\frac{\int\prod_{n=1}^{\infty}\mathrm{d}a_n\exp(\mathrm{i}ka_0)\exp\left(-\beta\frac{M}{4}\sum_{n=1}^{\infty}[\omega_n^2 + \Omega^2(x_c)]\left[a_n - \frac{1}{\beta M}\frac{2\mathrm{i}k\cos(\omega_n\tau)}{\omega_n^2 + \Omega^2(x_c)}\right]^2\right)}{\int\prod_{n=1}^{\infty}\mathrm{d}a_n\exp\left(-\beta\frac{M}{2}\sum_{n=1}^{\infty}[\omega_n^2 + \Omega^2(x_c)]\frac{a_n^2}{2}\right)} \times \exp\left(-\sum_{n=1}^{\infty}\frac{1}{\beta M}\frac{k^2\cos^2(\omega_n\tau)}{\omega_n^2 + \Omega^2(x_c)}\right) \tag{41}$$

or (see eq 33)

https://doi.org/10.1021/acs.jpca.1c05860
J. Phys. Chem. A 2021, 125, 9209−9225

$$\langle V(x(\tau))\rangle_{tr}^{x_c} = \frac{1}{2\pi}\int_{-\infty}^{\infty} dk\ \tilde{V}(k)\ \exp(ika_0) \times \exp\left(-\sum_{n=1}^{\infty}\frac{1}{\beta M}\frac{k^2\cos^2(\omega_n\tau)}{\omega_n^2+\Omega^2(x_c)}\right) = \frac{1}{2\pi}\int_{-\infty}^{\infty} dk\ \tilde{V}(k)\ \exp\left(ika_0 - \frac{1}{2}a^2(x_c,\tau)k^2\right) \tag{42}$$

Inserting the inverse Fourier transform of the potential $V(x)$

$$\tilde{V}(k) = \int_{-\infty}^{\infty} dx\ V(x)\ \exp(-ikx) \tag{43}$$

we obtain

$$\begin{aligned}&\langle V(x(\tau))\rangle_{tr}^{x_c}\\ &= \frac{1}{2\pi}\int_{-\infty}^{\infty} dx\ V(x)\int_{-\infty}^{\infty} dk\ \exp(-ikx)\ \exp\left(ika_0 - \frac{1}{2}a^2(x_c,\tau)k^2\right)\\ &= \frac{1}{2\pi}\int_{-\infty}^{\infty} dx\ V(x)\int_{-\infty}^{\infty} dk\ \exp\left(-\frac{1}{2}a^2(x_c,\tau)\left(k+\frac{i(x-a_0)}{a^2(x_c,\tau)}\right)^2 - \frac{(x-a_0)^2}{2a^2(x_c,\tau)}\right)\\ &= \left(\frac{1}{2\pi a^2(x_c,\tau)}\right)^{1/2}\int dx\ V(x)\ \exp\left(-\frac{(x-a_0)^2}{2a^2(x_c,\tau)}\right)\end{aligned} \tag{44}$$

This is a Gaussian smearing of the potential around the centroid $x_c = a_0$. We shall call it $V_{a^2(x_c,\tau)}(x_c)$. Hence,

$$\langle V(x(\tau))\rangle_{tr}^{x_c} = V_{a^2(x_c,\tau)}(x_c) \tag{45}$$

Equation 25 can now be written

$$\begin{aligned}&\langle S[x(\tau)] - S_{tr}^{x_c}[x(\tau)]\rangle_{tr}^{x_c}\\ &= \int_0^{\beta\hbar} d\tau\ \left\{\langle V(x(\tau))\rangle_{tr}^{x_c} - L(x_c) - \frac{1}{2}M\Omega^2(x_c)\langle(x(\tau)-x_c)^2\rangle_{tr}^{x_c}\right\}\\ &= -\beta\hbar L(x_c) + \int_0^{\beta\hbar} d\tau\ V_{a^2(x_c,\tau)}(x_c) - \frac{\beta\hbar}{2}M\Omega^2(x_c)a^2(x_c)\end{aligned} \tag{46}$$

Putting the pieces together, eq 23 becomes

$$\langle S[x(\tau)] - S_{tr}^{x_c}[x(\tau)]\rangle_{tr}^{x_c} = \frac{\int dx_c\ \Delta_{tr}(x_c) \times \left(-\beta\hbar L(x_c) + \int_0^{\beta\hbar} d\tau\ V_{a^2(x_c,\tau)}(x_c) - \frac{\beta\hbar}{2}M\Omega^2(x_c)\ a^2(x_c)\right)}{\int dx_c\ \Delta_{tr}(x_c)}$$

so that eq 21 becomes

$$\int dx_c\ \Delta(x_c) \geq \int dx_c'\ \exp(-\beta L(x_c'))\ \alpha(x_c') \times \exp\left(\frac{\int dx_c\ \exp(-\beta L(x_c))\ \alpha(x_c) \times \left(\beta L(x_c) + \frac{\beta}{2}M\Omega^2(x_c)\ a^2(x_c) - \int_0^{\beta\hbar} d\tau\ V_{a^2(x_c,\tau)}(x_c)/\hbar\right)}{\int dx_c''\ \alpha(x_c'')\ \exp(-\beta L(x_c''))}\right) \tag{47}$$

We call the right-hand side of this inequality $I = I[\Omega^2(x_c), L(x_c)]$. Thus, I is a functional of the functions $\Omega^2(x_c)$ and $L(x_c)$. We need to make it stationary with respect to variations in $L(x_c)$ and $\Omega^2(x_c)$ for all values of x_c. First we will determine the potential $L(x_c)$ by requiring

$$L(x_c) = \frac{1}{\beta\hbar}\int_0^{\beta\hbar} d\tau\ V_{a^2(x_c,\tau)}(x_c) - \frac{1}{2}M\Omega^2(x_c)\ a^2(x_c) \tag{48}$$

With this choice, consider the functional variation with respect to $L(x_c)$. The variation vanishes since

$$\delta I = \int dx_c'\ [-\beta\delta L(x_c')\ \exp(-\beta L(x_c'))\ \alpha(x_c')] + \int dx_c'\ \exp(-\beta L(x_c'))\ \alpha(x_c') \times \int dx_c\ \frac{\exp(-\beta L(x_c))\ \alpha(x_c)(\beta\delta L(x_c))}{\int dx_c''\ \alpha(x_c'')\ \exp(-\beta L(x_c''))} = 0 \tag{49}$$

Next we turn to the variation of $\Omega^2(x_c)$. The right-hand side depends directly on $\Omega^2(x_c)$ but also indirectly through $a^2(x_c)$, $\alpha(x_c)$, and $\int_0^{\beta\hbar} d\tau\ V_{a^2(x_c,\tau)}(x_c)/\hbar$. Hence there are four contributions to changes in I when varying $\Omega^2(x_c)$. The functional derivative of I with respect to $\Omega^2(x_c)$ is

$$\frac{\delta I}{\delta\Omega^2(x_c)} = \exp(-\beta L(x_c))\ \alpha(x_c) \times \frac{\beta}{2}Ma^2(x_c) \tag{50}$$

Next, we calculate the result of variations in $\Omega^2(x_c)$ coming from $a^2(x_c)$. We write it symbolically

$$\frac{\delta I}{\delta a^2(x_c)}\frac{\delta a^2(x_c)}{\delta\Omega^2(x_c)} = \exp(-\beta L(x_c))\ \alpha(x_c) \times \frac{\beta}{2}M\Omega^2(x_c) \times \frac{\partial a^2(x_c)}{\partial\Omega^2(x_c)} \tag{51}$$

The third term is

$$\frac{\delta I}{\delta\alpha(x_c)}\frac{\delta\alpha(x_c)}{\delta\Omega^2(x_c)} = \exp(-\beta L(x_c))\frac{\partial\alpha(x_c)}{\partial\Omega^2(x_c)} \tag{52}$$

Finally, the fourth term is

$$\frac{\delta I}{\delta\int_0^{\beta\hbar} d\tau\ V_{a^2(x_c,\tau)}(x_c)}\frac{\delta\int_0^{\beta\hbar} d\tau\ V_{a^2(x_c,\tau)}(x_c)}{\delta\Omega^2(x_c)} = -\exp(-\beta L(x_c))\ \alpha(x_c) \times \frac{\partial\int_0^{\beta\hbar} d\tau\ V_{a^2(x_c,\tau)}(x_c)/\hbar}{\partial\Omega^2(x_c)} \tag{53}$$

https://doi.org/10.1021/acs.jpca.1c05860
J. Phys. Chem. A 2021, 125, 9209−9225

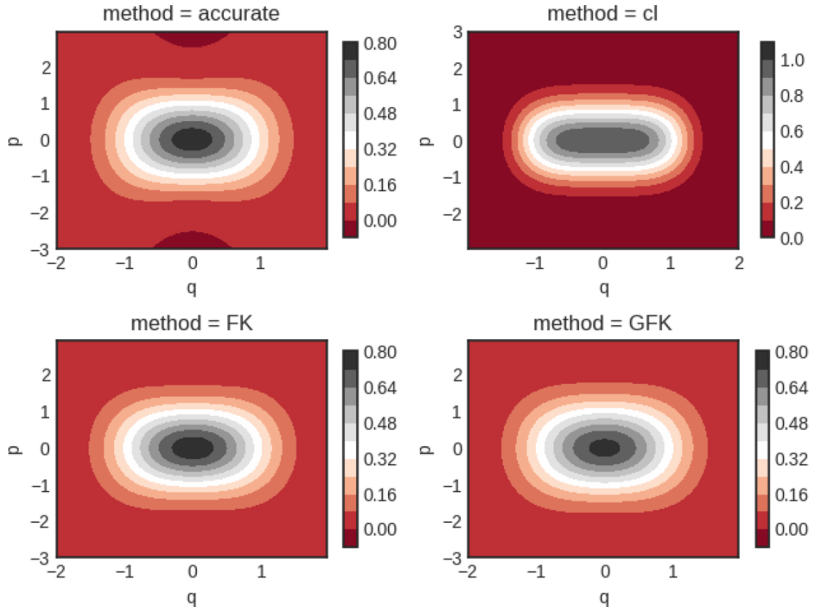

Figure 1. Quartic oscillator Wigner functions for $\beta = 2$. Notice the different scale for the classical calculation (cl).

The sum of these four terms must vanish. As we shall see, we can make the first and third terms sum to zero. Likewise with the second and fourth. Looking at the first pair, we get

$$\alpha(x_c) \times \frac{\beta}{2} M a^2(x_c) = -\frac{\partial \alpha(x_c)}{\partial \Omega^2(x_c)}$$
$$\Leftrightarrow a^2(x_c) = -\frac{2}{M\beta}\frac{\partial \ln \alpha(x_c)}{\partial \Omega^2(x_c)} \tag{54}$$

We already have expressions for $a^2(x_c)$ and $\alpha(x_c)$ in eqs 39 and 22, respectively. From these we can verify that eq 54 is fulfilled.

Next, let us look at the sum of the second and fourth terms. The equation we get is

$$\frac{\beta}{2} M\Omega^2(x_c) \times \frac{\partial a^2(x_c)}{\partial \Omega^2(x_c)} = \frac{\partial \int_0^{\beta\hbar} d\tau\, V_{a^2(x_c,\tau)}(x_c)/\hbar}{\partial \Omega^2(x_c)} \tag{55}$$

Using the chain rule, we may write

$$\frac{\beta}{2} M\Omega^2(x_c) \times \frac{\partial a^2(x_c)}{\partial \Omega^2(x_c)} = \int_0^{\beta\hbar} d\tau\, \frac{\partial a^2(x_c,\tau)}{\partial \Omega^2(x_c)} \frac{\partial V_{a^2(x_c,\tau)}(x_c)}{\partial a^2(x_c,\tau)}/\hbar \tag{56}$$

Since $a^2(x_c)$ is the path-averaged smearing width, we have

$$a^2(x_c) = \frac{1}{\beta\hbar}\int_0^{\beta\hbar} d\tau\, \langle (x(\tau) - x_c)^2 \rangle_{tr}^{x_c} = \frac{1}{\beta\hbar}\int_0^{\beta\hbar} d\tau\, a^2(x_c,\tau) \tag{57}$$

Thus, we may write

$$\frac{\partial a^2(x_c)}{\partial \Omega^2(x_c)} = \frac{1}{\beta\hbar}\int_0^{\beta\hbar} d\tau\, \frac{\partial a^2(x_c,\tau)}{\partial \Omega^2(x_c)} \tag{58}$$

Equation 56 therefore finally becomes

$$\Omega^2(x_c) = \frac{2}{\hbar M\beta}\frac{\int_0^{\beta\hbar} d\tau\, \frac{\partial a^2(x_c,\tau)}{\partial \Omega^2(x_c)} \frac{\partial V_{a^2(x_c,\tau)}(x_c)}{\partial a^2(x_c,\tau)}}{\frac{1}{\beta\hbar}\int_0^{\beta\hbar} d\tau\, \frac{\partial a^2(x_c,\tau)}{\partial \Omega^2(x_c)}} = \frac{1}{M}\frac{\int_0^{\beta\hbar} d\tau\, \frac{\partial a^2(x_c,\tau)}{\partial \Omega^2(x_c)} V''_{a^2(x_c,\tau)}(x_c)}{\int_0^{\beta\hbar} d\tau\, \frac{\partial a^2(x_c,\tau)}{\partial \Omega^2(x_c)}} \tag{59}$$

where we have utilized the equality

$$2\frac{\partial V_{a^2(x_c,\tau)}(x_c)}{\partial a^2(x_c,\tau)} = V''_{a^2(x_c,\tau)}(x_c) \tag{60}$$

which follows from manipulations on eq 44.

Equation 59 is our iterative equation which is used together with the expression for $a^2(x_c, \tau)$ in eq 36. The iteration starts by first fixing a centroid x_c and choosing a value for $\Omega^2(x_c)$. Iteration then goes on until convergence.

In eq 59 we need to evaluate $\partial a^2(x_c, \tau)/\partial \Omega^2(x_c)$. By differentiating eq 36, the following expression may be found

$$\frac{\partial a^2(x_c,\tau)}{\partial \Omega^2(x_c)} = \frac{\hbar^3\beta^2}{16M\Omega(x_c)} \times \frac{\frac{2}{y} - \coth(y) - \frac{y}{\sinh^2(y)}}{y^2} + \left\{\frac{\hbar \sinh^2\left(\hbar\Omega(x_c)\left(\tau - \frac{\beta}{2}\right)\right)}{2M\Omega(x_c)^3 \sinh(\hbar\Omega(x_c)\beta)}\right\} \times \left\{2\hbar\Omega(x_c)\left(\tau - \frac{\beta}{2}\right)\coth\left(\hbar\Omega(x_c)\left(\tau - \frac{\beta}{2}\right)\right) - \hbar\Omega(x_c)\beta\coth(\hbar\Omega(x_c)\beta) - 1\right\} \tag{61}$$

where we have set $\hbar\Omega(x_c)\beta/2 = y$ for brevity.

For the case of an imaginary frequency, the expressions for $a^2(x_c, \tau)$, $a^2(x_c)$, and $\partial a^2(x_c, \tau)/\partial \Omega^2(x_c)$ change. By replacing $\Omega(x_c)$ with $i|\Omega(x_c)|$, the new expressions become

https://doi.org/10.1021/acs.jpca.1c05860
J. Phys. Chem. A 2021, 125, 9209−9225

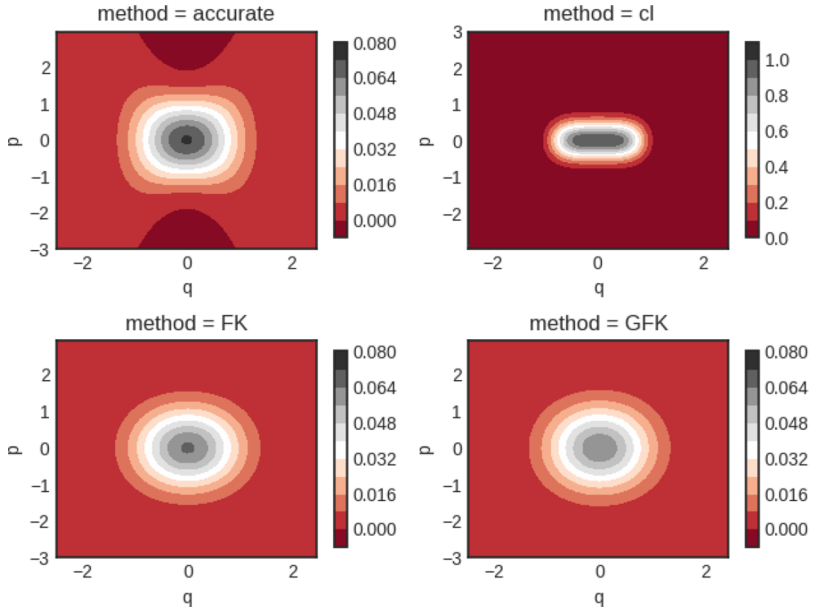

Figure 2. Quartic oscillator Wigner functions for $\beta = 8$. Notice the different scale for the classical calculation (cl).

$$a^2(x_c, \tau) = {a_{FK}}^2(x_c) + \frac{\hbar}{M|\Omega(x_c)|}\frac{\sin^2(|\Omega(x_c)|(\beta\hbar/2 - \tau))}{\sin(|\Omega(x_c)|\beta\hbar)} \tag{62}$$

$$a^2(x_c) = {a_{FK}}^2(x_c) + \frac{\beta\hbar|\Omega(x_c)| - \sin(\beta\hbar|\Omega(x_c)|)}{2\beta M\,|\Omega(x_c)|^2\,\sin(\hbar|\Omega(x_c)|\beta)} \tag{63}$$

and

$$\begin{aligned}\frac{\partial a^2(x_c, \tau)}{\partial \Omega^2(x_c)} = {}& \frac{\hbar^3\beta^2}{16M|\Omega(x_c)|} \times \frac{\frac{2}{|y|} - \cot(|y|) - \frac{|y|}{\sin^2(|y|)}}{|y|^2} \\ & - \frac{\hbar\,\sin^2\left(\hbar|\Omega(x_c)|\left(\tau - \frac{\beta}{2}\right)\right)}{2M\,|\Omega(x_c)|^3\,\sin(\hbar|\Omega(x_c)|\beta)}\left\{2\hbar|\Omega(x_c)|\left(\tau - \frac{\beta}{2}\right)\right. \\ & \left.\times \cot\left(\hbar|\Omega(x_c)|\left(\tau - \frac{\beta}{2}\right)\right)\right. \\ & \left. - \hbar|\Omega(x_c)|\beta\,\cot(\hbar|\Omega(x_c)|\beta) - 1\right\}, \qquad |y| = \frac{\hbar|\Omega(x_c)|\beta}{2}\end{aligned} \tag{64}$$

Here

$$\begin{aligned}&{a_{FK}}^2(x_c) \\ &= \frac{1}{M\,|\Omega(x_c)|^2\beta}\left\{1 - \frac{\hbar|\Omega(x_c)|\beta}{2}\,\cot\left(\frac{\hbar|\Omega(x_c)|\beta}{2}\right)\right\}\end{aligned} \tag{65}$$

RESULTS

We will apply our new effective frequency theory to two problems, viz. a quartic oscillator and a symmetric double well. The results will be compared with predictions from the original effective frequency theory, classical statistical mechanics as well as accurate calculations. We will use natural units so that $\hbar = 1$ and we consider a particle with mass $m = 1$.

The Quartic Oscillator. Here we consider a quartic potential $V(q) = q^4/4$. In this case we do not encounter any imaginary frequency problem. Hence, the original effective frequency theory is always well-defined. The inverse temperatures that we study are $\beta = 2$ and 8. In Figure 1, computed Wigner functions are shown for $\beta = 2$ obtained from an accurate calculation, a classical calculation, and the original and new effective frequency models, termed FK and GFK, respectively.

Notice that the Wigner functions are not normalized to unity when integrated. They are Wigner transforms of the Boltzmann operator itself. In Figure 1 good agreement is seen between all four predictions, albeit the classical calculation yields clear deviations from the other results.

The results for the case $\beta = 8$ are shown in Figure 2.

It is clearly seen that the classical result shows large deviation from the other three results. Visually, the two effective frequency theories agree well with each other and also with the accurate quantum result.

In order to make the comparisons between methods more precise, we have adopted the following measure of deviation of an approximate Wigner function, $W(q, p)$, from the accurate Wigner function $W_{acc}(q, p)$:

$$\begin{aligned}&\text{error}[W(q, p), W_{acc}(q, p)] \\ &= \left(\frac{\iint \mathrm{d}q\,\mathrm{d}p\,(W(q, p) - W_{acc}(q, p))^2}{\iint \mathrm{d}q\,\mathrm{d}p\,W_{acc}(q, p)^2}\right)^{1/2}\end{aligned} \tag{66}$$

In Table 1 such error values are shown for the quartic oscillator at both $\beta = 2$ and $\beta = 8$.

Table 1. Quartic Potential[a]

	FK	GFK	Cl
$\beta = 2$	0.02	0.03	0.44
$\beta = 8$	0.07	0.10	9.47

[a]Deviations from the accurate Wigner function are shown for original Feynman−Kleinert effective frequency theory (FK), our generalized effective frequency theory (GFK) and classical theory (Cl).

https://doi.org/10.1021/acs.jpca.1c05860
J. Phys. Chem. A 2021, 125, 9209−9225

It is again confirmed that the two effective frequency theories are very close to each other. Moments of the Wigner functions are presented in Table 2.

Table 2. Quartic Oscillator[a]

	FK	GFK	accurate	Cl
$\langle q^2\rangle$, $\beta = 2$	0.53	0.53	0.53	0.48
$\langle p^2\rangle$, $\beta = 2$	0.73	0.79	0.73	0.50
$\langle q^2\rangle$, $\beta = 8$	0.45	0.43	0.46	0.24
$\langle p^2\rangle$, $\beta = 8$	0.57	0.61	0.56	0.12

[a]Moments of the Wigner function from original Feynman−Kleinert effective frequency theory (FK), our generalized effective frequency theory (GFK), accurate calculations and classical theory (Cl).

Compared to the accurate calculations and original effective frequency model, the new theory is seen to give slightly larger momenta as the temperature is lowered, while the classical ones are clearly too small.

We will now consider the off-diagonal behavior of the density matrix, i.e., how η behaves in $\left\langle q - \frac{\eta}{2}\middle|\hat{\rho}\middle|q + \frac{\eta}{2}\right\rangle$. We define

$$\langle \eta^2\rangle = \frac{\iint \mathrm{d}q\ \mathrm{d}\eta\ \eta^2 \langle q - \frac{\eta}{2}|\hat{\rho}|q + \frac{\eta}{2}\rangle}{\iint \mathrm{d}q\ \mathrm{d}\eta\ \langle q - \frac{\eta}{2}|\hat{\rho}|q + \frac{\eta}{2}\rangle} \tag{67}$$

and show the corresponding values in Table 3 for FK, GFK, and accurate calculations.

Table 3. Quartic Oscillator[a]

	FK	GFK	accurate
$\langle \eta^2\rangle$ $\beta = 2$	1.45	1.32	1.32
$\langle \eta^2\rangle$ $\beta = 8$	1.77	1.66	1.59

[a]$\langle \eta^2\rangle$ of the density matrix from the original Feynman−Kleinert effective frequency theory (FK), our generalized effective frequency theory (GFK) and accurate calculations.

The off-diagonal behavior of the density matrix is seen to be better for GFK than for FK.

We end this section by showing the position autocorrelation functions, obtained by running classical dynamics using our Wigner functions to sample initial conditions (often referred to as the "Classical Wigner" model). In Figures 3 and 4 we show results for $\beta = 2$ and 8, respectively. The figures also contain accurate and purely classical dynamics results. The results from the two effective frequency theories are practically speaking identical.

Particle in a Double Well. We now turn to a problem with a barrier, namely, the double well, and we choose the potential to be $V(q) = -\frac{1}{2}q^2 + \frac{1}{10}q^4$. The double well problem is substantially more challenging than what the quartic potential is. For this potential the momentum part of the Wigner function of the original effective frequency theory becomes ill-defined in the interval $\beta \in [5.1, 5.9]$. We therefore choose to consider inverse temperatures outside, but reasonably close to, this range. We also consider the results of the so-called local Gaussian approximation (LGA) proposed by Liu and Miller.[12] This scheme utilizes the following approximation to the Boltzmann operator Wigner transform:

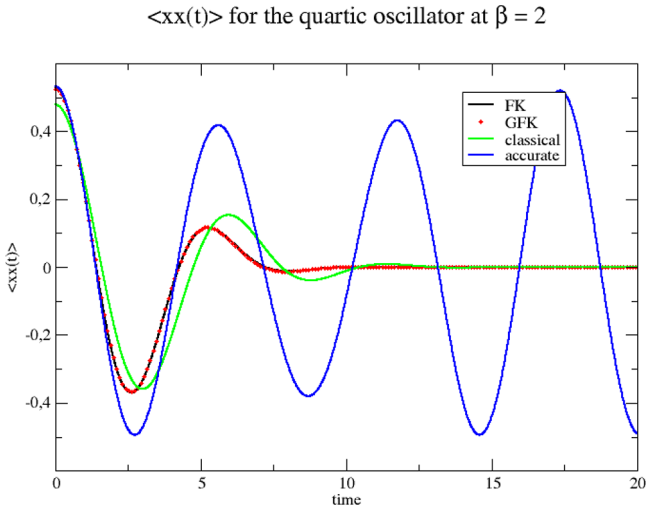

Figure 3. Correlation functions for the quartic oscillator at $\beta = 2$. The three Wigner functions used as sampling functions for initiating the classical dynamics are derived from the original Feynman−Kleinert effective frequency theory (FK), our generalized effective frequency theory (GFK), and classical statistical mechanics (classical). Accurate quantum mechanical results are also shown (accurate).

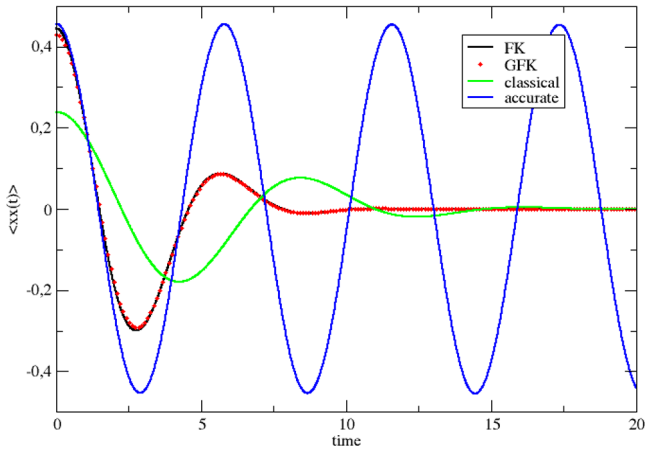

Figure 4. Correlation functions for the quartic oscillator at $\beta = 8$. The three Wigner functions used as sampling functions for initiating the classical dynamics are derived from the original Feynman−Kleinert effective frequency theory (FK), our generalized effective frequency theory (GFK), and classical statistical mechanics (classical). Accurate quantum mechanical results are also shown (accurate).

$$P(x, p) \approx \langle x|\exp(-\beta\hat{H})|x\rangle \times \sqrt{\frac{\beta\hbar}{mQ(u(x))}}\exp\left(-\frac{\beta}{2mQ(u(x))}p^2\right) \tag{68}$$

where $u(x)$ is the local frequency $u(x)^2 = V''(x)/m$ and $Q(u(x))$ is given by

$$Q(u(x)) = \begin{cases} \dfrac{\beta\hbar u(x)/2}{\tanh(\beta\hbar u(x)/2)}, & u(x)^2 \geq 0 \\ \dfrac{\tanh(\beta\hbar|u(x)|/2)}{\beta\hbar|u(x)|/2}, & u(x)^2 < 0 \end{cases} \tag{69}$$

https://doi.org/10.1021/acs.jpca.1c05860
J. Phys. Chem. A 2021, 125, 9209−9225

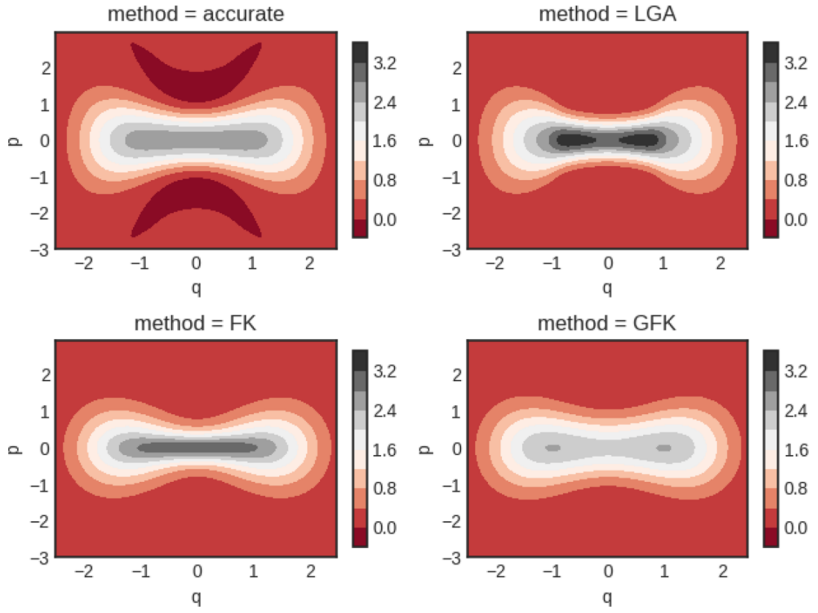

Figure 5. Double well Wigner functions for $\beta = 4$. Although not shown, the classical Wigner function has a peak value of around 13.5.

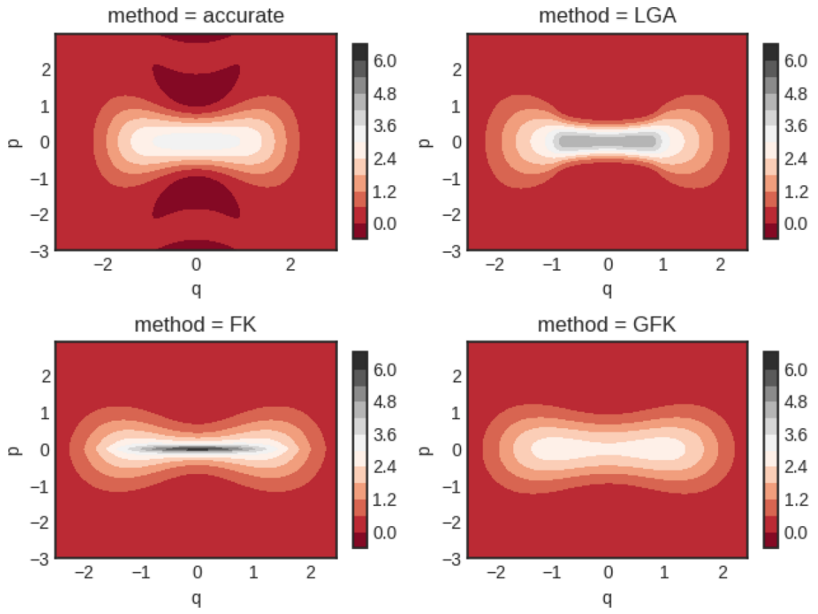

Figure 6. Double well Wigner functions for $\beta = 5$. Although not shown, the classical Wigner function has a peak value of around 25.

Equation 68 is always well-defined. Also, the phase-space trace of $P(x, p)$ is exact so the Wigner function is correctly normalized. In Figures 5−7 we show the Wigner distributions for $\beta = 4$, 5, and 8, respectively, for the four methods that we compare, namely, accurate, FK, GFK, and LGA.

For $\beta = 4$, it is seen that the Wigner function derived from the original Feynman−Kleinert theory possesses a too narrow momentum distribution near the barrier top in comparison to the accurate result. The situation is similar for the LGA Wigner function. Both of these functions also have a too large maximum value of $P(x, p)$. In comparison, the GFK function behaves better. In the case of $\beta = 5$, where $\hbar|\Omega(x_c)|\beta$ is closer to π, the same observations hold but they are more accentuated. For $\beta = 8$, the LGA Wigner function decays very rapidly along the p axis and deviates substantially from the accurate one.

It is hard to judge how close the approximate Wigner functions are to the accurate one. The comparison is further complicated by the fact that only the exact function can be negative. Again we may turn to our error estimate. In Table 4, we present error values calculated using eq 66.

Again we see that the results for the two effective frequency theories are quite close to each other and much better than the classical results. Note that for $\beta = 5$, as opposed to for the other β-values, FK is sligthly worse than GFK. This is because $\beta = 5$ is quite close to the β-range where FK becomes ill-defined. The LGA approximation is seen to perform slightly worse than the two effective frequency theories.

We may also consider moments of the Wigner function; see Table 5.

The original Feynman−Kleinert effective frequency theory is seen to give results quite close to the accurate ones. Our new

https://doi.org/10.1021/acs.jpca.1c05860
J. Phys. Chem. A 2021, 125, 9209−9225

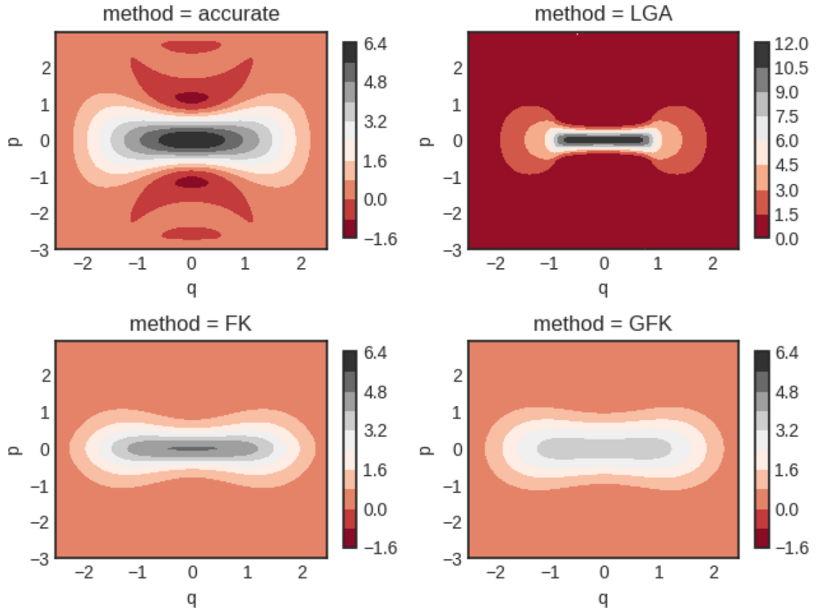

Figure 7. Double well Wigner functions for $\beta = 8$. Notice the different scale for the LGA calculation. Although not shown, the classical Wigner function has a peak value of around 150.

Table 4. Double Well Results[a]

	FK	GFK	LGA	Cl
$\beta = 4$	0.14	0.14	0.16	2.0
$\beta = 5$	0.26	0.18	0.25	3.4
$\beta = 8$	0.28	0.35	0.52	12
$\beta = 10$	0.35	0.42	0.67	29

[a]Deviations from accurate Wigner function results calculated from eq 66. Results are shown for the original Feynman−Kleinert effective frequency theory (FK), our generalized effective frequency theory (GFK), local Gaussian approximation (LGA),[12] and purely classical theory (Cl).

Table 5. Double Well Results for Moments of the Wigner Functions[a]

	FK	GFK	LGA	accurate	Cl
$\langle q^2\rangle$, $\beta = 4$	1.71	1.66	1.71	1.71	2.18
$\langle p^2\rangle$, $\beta = 4$	0.48	0.54	0.48	0.49	0.25
$\langle q^2\rangle$, $\beta = 5$	1.65	1.59	1.65	1.65	2.23
$\langle p^2\rangle$, $\beta = 5$	0.44	0.51	0.44	0.44	0.20
$\langle q^2\rangle$, $\beta = 8$	1.53	1.48	1.55	1.55	2.34
$\langle p^2\rangle$, $\beta = 8$	0.40	0.46	0.39	0.36	0.12
$\langle q^2\rangle$, $\beta = 10$	1.47	1.43	1.52	1.52	2.38
$\langle p^2\rangle$, $\beta = 10$	0.39	0.44	0.37	0.33	0.10

[a]Results are shown for the original Feynman−Kleinert effective frequency theory (FK), our generalized effective frequency theory (GFK), local Gaussian approximation (LGA),[12] accurate calculations, and classical theory (Cl).

method systematically slightly overestimates the momentum of the system and similarly slightly underestimates $\langle q^2\rangle$, while the classical results are substantially worse. The LGA approximation is clearly seen to work well. In fact, the LGA model predicts the most correct moments, being slightly closer to the accurate ones than the original FK model.

In Table 6 we show the average value of η^2 for the double well at various temperatures. When β is near the interval $[5.1, 5.9]$, we see the divergence behavior in $\langle\eta^2\rangle$ as obtained from

Table 6. Double Well Results for $\langle\eta^2\rangle$ of the Density Matrix[a]

	FK	GFK	LGA	accurate
$\langle\eta^2\rangle$, $\beta = 4$	6.72	2.36	3.68	2.63
$\langle\eta^2\rangle$, $\beta = 5$	133	2.53	5.14	2.97
$\langle\eta^2\rangle$, $\beta = 6$	106	2.63	6.97	3.22
$\langle\eta^2\rangle$, $\beta = 8$	7.13	2.76	11.79	3.56

[a]Results are shown from original Feynman−Kleinert effective frequency theory (FK), our generalized effective frequency theory (GFK), local Gaussian approximation (LGA),[12] and accurate calculation.

FK theory. Also, the LGA approximation performs poorly: It predicts too large values of $\langle\eta^2\rangle$ which is equivalent to a very slowly decaying density matrix in its off-diagonal direction. The GFK model predicts values of $\langle\eta^2\rangle$ being in much better agreement with the accurate values. Thus, the GFK method outperforms the LGA and original effective frequency model when it comes to predicting the off-diagonal behavior of the density matrix.

As in the previous section, we show the position autocorrelation functions, obtained from the Classical Wigner model. This is done in Figures 8 and 9 for $\beta = 4$ and 8, respectively.

The results for the two effective frequency theories and the LGA result agree quite well with each other. They are all clearly better than the classical results. We conclude that it does not matter which of the three theories you adopt for the position autocorrelation functions. Due to the Classical Wigner model itself, the results obtained are essentially equally far away from the accurate result.

DISCUSSION AND CONCLUSIONS

A new effective frequency model for imaginary time path integrals has been proposed. Since the new theory is a generalization of the Feynman−Kleinert (FK) theory in that it also includes open paths, we term it the Generalized Feynman−Kleinert theory (GFK). More specifically, GFK

https://doi.org/10.1021/acs.jpca.1c05860
J. Phys. Chem. A 2021, 125, 9209−9225

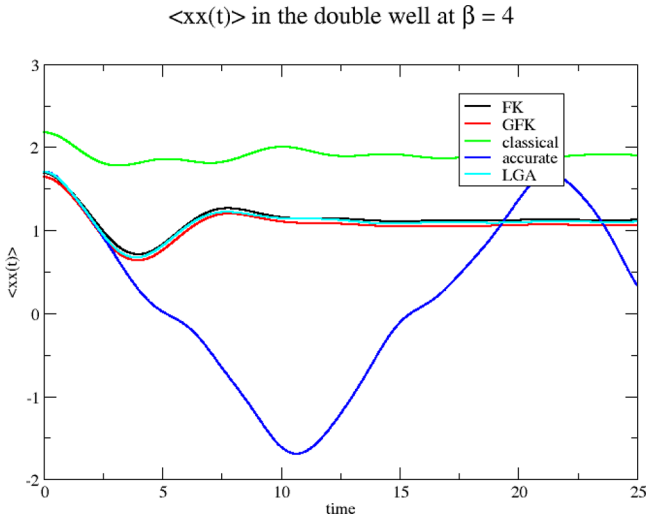

Figure 8. Position autocorrelation functions for the double well at β = 4. The four Wigner functions used as sampling functions for initiating the classical dynamics are derived from the original Feynman−Kleinert effective frequency theory (FK), our generalized effective frequency theory (GFK), local Gaussian approximation (LGA), and classical statistical mechanics (classical). Accurate quantum mechanical results are also shown (accurate).

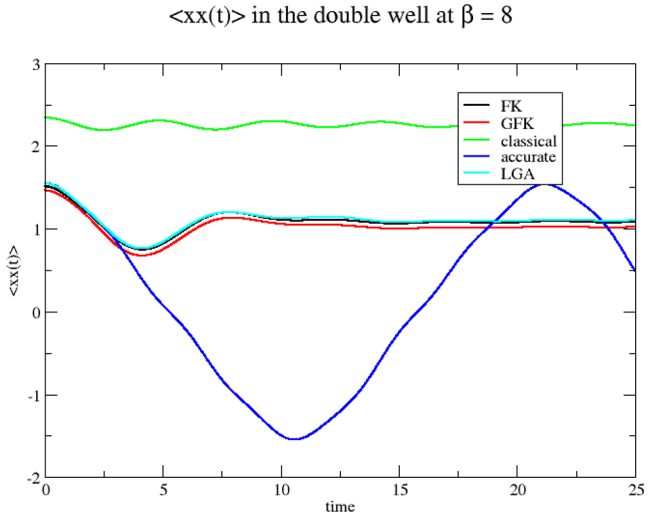

Figure 9. Position autocorrelation functions for the double well at β = 8. The four Wigner functions used as sampling functions for initiating the classical dynamics are derived from the original Feynman−Kleinert effective frequency theory (FK), our generalized effective frequency theory (GFK), local Gaussian approximation (LGA), and classical statistical mechanics (classical). Accurate quantum mechanical results are also shown (accurate).

"trains" the effective frequency trial action also on open paths as opposed to the original model which was developed for closed paths only. This removed the divergence problem inherent in the original Feynman−Kleinert theory, when obtaining the Wigner functions for barrier problems. The inclusion of open paths in the variational procedure was shown to lead to a more accurate off-diagonal behavior of the density matrix. The GFK theory is, however, not generally more accurate than the original closed-path model of Feynman−Kleinert. On the contrary, it was seen to provide quadratic moments that are slightly worse than those predicted from the original FK model (and LGA model as well).

What are the reasons for the observations mentioned just above? We first point out that the two effective frequency theories utilize the same trial action. GFK is thus not more elaborate. It, however, "trains" its trial action on a larger class of paths. It is therefore not surprising that when comparing moments such as, e.g., $\langle x^2 \rangle$ and $\langle p^2 \rangle$, which may be calculated using only *closed* paths, the FK theory is more precise, since it is optimized for precisely such paths. The present study, however, suggests that when calculating such quantities the differences between the two models are very small. On the other hand, in studying quantities depending on the off-diagonal behavior of the density matrix, GFK outperforms FK for temperatures close to where the FK theory leads to divergence issues.

The results of this paper, suggest that the GFK theory provides a "Jack of all trades" Wigner transform approach, since its density matrix and Wigner transform plots are always consistent (but not always the most accurate). This should be contrasted to the FK theory with its divergence issues and the LGA model which predicts an errorneous rapid decay of its double well Wigner function along the momentum axis.

We end by pointing out immediate possible generalizations. Instead of including just the centroid, we could include additional Fourier modes in the anharmonic part of the trial action. For instance, we could choose to use the two lowest modes a_0 and a_1, which turns the trial action into

$$S_{tr}^{(a_0,a_1)}[x(\tau)] = \int_0^{\beta\hbar} d\tau \left\{ \frac{M}{2}\dot{x}(\tau)^2 + V_{\Omega(a_0,a_1),L(a_0,a_1)}(x(\tau)) \right\} \tag{70}$$

where

$$V_{\Omega(a_0,a_1),L(a_0,a_1)}(x(\tau)) = L(a_0, a_1) + \frac{1}{2}M\Omega^2(a_0, a_1)(x(\tau) - a_0 - a_1 \cos(\omega_1\tau))^2 \tag{71}$$

This is a generalization of eq 13. Thus, the action is now expanded harmonically around a *time-dependent* path $y(\tau) = a_0 + a_1 \cos(\omega_1\tau)$; see Figure 10.

All developments proceed essentially as before and the required expressions can be calculated with the path integral technique outlined in Appendix B.

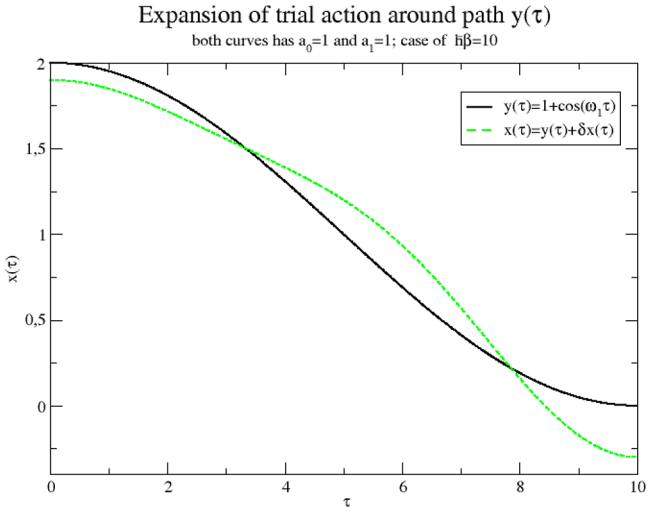

Figure 10. Trial action $x(\tau)$ expanded around a path $y(\tau)$.

https://doi.org/10.1021/acs.jpca.1c05860
J. Phys. Chem. A 2021, 125, 9209−9225

By proceeding as just outlined but including more and more modes, the trial action approaches the exact action. In multidimensional applications, we could apply this multimode theory to the most important degrees of freedom, but use the single mode version detailed in this paper for the other degrees of freedom. Further, we could apply similar ideas as presented here for developing trial actions for path integrals involving thermalized flux operators. In this case, besides the centroid, we would impose further constraints on the open paths by requiring the paths to pass the dividing surface at $\tau = \beta\hbar/2$; see, e.g., refs 4 and 28. As shown in the Supporting Information, such further restrictions can be implemented by inserting delta functions into the off-diagonal path integral.

APPENDIX A

Miscellaneous Results

The purpose of this appendix is to derive eqs 10, 22, and 35. We first derive eq 10. We start from eq 10 in ref 23 which gives the Feynman−Kleinert approximation to the Wigner transform of the Boltzmann operator. It reads

$$\begin{aligned}(\exp(-\beta\hat{H}))_W[q,p] &= \int \frac{dx_c}{2\pi\hbar}\exp(-\beta W(x_c)) \times \frac{2}{\alpha}\left(\frac{M\alpha\pi}{\frac{\beta}{2}\coth(\hbar\Omega(x_c)\beta/2)}\right)^{1/2} \\ &\quad \times \exp\left(-\frac{M\Omega(x_c)}{\hbar\alpha}(q-x_c)^2 - \frac{\tanh(\hbar\Omega(x_c)\beta/2)}{M\Omega(x_c)\hbar}p^2\right) \\ &= \int \frac{dx_c}{\pi\hbar}\exp(-\beta W(x_c)) \times \left(\frac{\pi\hbar\tanh(\hbar\Omega(x_c)\beta/2)}{\beta\Omega(x_c){a_{FK}}^2(x_c)}\right)^{1/2} \\ &\quad \times \exp\left(-\frac{1}{2}\frac{1}{{a_{FK}}^2(x_c)}(q-x_c)^2 - \frac{\tanh(\hbar\Omega(x_c)\beta/2)}{M\Omega(x_c)\hbar}p^2\right)\end{aligned} \tag{72}$$

where $\alpha = \alpha(x_c)$ is related to the Feynman−Kleinert smearing width by $\alpha = 2M\Omega(x_c){a_{FK}}^2(x_c)/\hbar$. The centroid potential is $W(x_c) = L(x_c) + \frac{1}{\beta}\ln\frac{\sinh(\hbar\Omega(x_c)\beta/2)}{\hbar\Omega(x_c)\beta/2}$.

Let $\hat{\Delta}_{tr}(x_c)$ denote the operator you get from $\hat{\Delta}(x_c)$ by replacing the true potential by the Feynman−Kleinert trial potential in eq 9. From the definition of $\hat{\Delta}(x_c)$ in eq 8, it follows that by adopting the FK trial potential

$$(\exp(-\beta\hat{H}))_W[q,p] = \int dx_c\ (\hat{\Delta}_{tr}(x_c))_W[q,p] \tag{73}$$

and so by comparing with eq 72 we get

$$\begin{aligned}(\hat{\Delta}_{tr}(x_c))_W[q,p] &= \frac{\exp(-\beta W(x_c))}{\pi\hbar} \\ &\quad \times \left(\frac{\pi\hbar\tanh(\hbar\Omega(x_c)\beta/2)}{\beta\Omega(x_c){a_{FK}}^2(x_c)}\right)^{1/2} \times \exp\left(-\frac{1}{2}\frac{1}{{a_{FK}}^2(x_c)}(q-x_c)^2\right. \\ &\quad \left. - \frac{\tanh(\hbar\Omega(x_c)\beta/2)}{M\Omega(x_c)\hbar}p^2\right)\end{aligned} \tag{74}$$

which is eq 10.

We next derive eq 22. By performing an inverse Wigner transform on eq 74, we get

$$\begin{aligned}\langle x'|\hat{\Delta}_{tr}(x_c)|x\rangle &= \int \frac{dp}{2\pi\hbar}\exp\left(\frac{-ip(x-x')}{\hbar}\right)(\hat{\Delta}_{tr}(x_c))_W[q,p] \\ &= \frac{1}{2\pi\hbar}\exp(-\beta W(x_c))\left(\frac{M}{{a_{FK}}^2(x_c)\beta}\right)^{1/2} \\ &\quad \times \exp\left(-\frac{1}{2{a_{FK}}^2(x_c)}\left(\frac{x+x'}{2}-x_c\right)^2\right. \\ &\quad \left. - \frac{M\Omega(x_c)}{4\tanh\left(\frac{\hbar}{2}\beta\Omega(x_c)\right)\hbar}(x'-x)^2\right)\end{aligned} \tag{75}$$

The off-diagonal trace is just integrating $\langle x'|\hat{\Delta}_{tr}(x_c)|x\rangle$ over both x and x'. The result is eq 22.

Finally we derive eq 35. By combining eqs 33 and 34, we obtain

$$\begin{aligned}\langle x^2(\tau)\rangle^{tr} &= {x_c}^2 - \frac{1}{2\beta M\Omega^2(x_c)} \\ &\quad + \frac{\hbar}{2M\Omega(x_c)}\frac{\cosh(\Omega(x_c)(\beta\hbar-2\tau))}{\sinh(\Omega(x_c)\beta\hbar)} \\ &\quad + \frac{1}{2M\Omega^2(x_c)\beta}(\hbar\Omega(x_c)\beta\coth(\Omega(x_c)\beta\hbar)-1)\end{aligned} \tag{76}$$

Using $\coth(x) = \coth(x/2) - 1/\sinh(x)$, we rewrite the third line so that

$$\begin{aligned}\langle x^2(\tau)\rangle^{tr} &= {x_c}^2 - \frac{1}{2\beta M\Omega^2(x_c)} \\ &\quad + \frac{\hbar}{2M\Omega(x_c)}\frac{\cosh(2\Omega(x_c)(\beta\hbar/2-\tau))}{\sinh(\Omega(x_c)\beta\hbar)} \\ &\quad + \frac{\hbar}{M\Omega^2(x_c)\beta}\left\{\frac{\hbar\Omega(x_c)\beta}{2}\coth(\Omega(x_c)\beta\hbar/2)-1\right\} \\ &\quad - \frac{\hbar}{2M\Omega(x_c)\sinh(\Omega(x_c)\beta\hbar)} + \frac{1}{2\beta M\Omega^2(x_c)} \\ &= {x_c}^2 + \frac{\hbar}{2M\Omega(x_c)}\frac{\cosh(2\Omega(x_c)(\beta\hbar/2-\tau))}{\sinh(\Omega(x_c)\beta\hbar)} + {a_{FK}}^2(x_c) \\ &\quad - \frac{\hbar}{2M\Omega(x_c)\sinh(\Omega(x_c)\beta\hbar)}\end{aligned} \tag{77}$$

Here the old smearing width from the original Feynman−Kleinert theory has appeared. It is

$${a_{FK}}^2(x_c) = \frac{\hbar}{M\Omega^2(x_c)\beta}\left\{\frac{\hbar\Omega(x_c)\beta}{2}\coth(\Omega(x_c)\beta\hbar/2)-1\right\}$$

and fulfils $\langle x^2(\tau)\rangle_{tr} = {a_{FK}}^2(x_c) + {x_c}^2$ if only closed paths are considered. The first part of eq 77 can be simplified by using $\cosh(2x) = 2\cosh^2(x) - 1 = 1 + 2\sinh^2(x)$. We then have

$$\begin{aligned}\langle x^2(\tau)\rangle_{tr} &= {x_c}^2 + \frac{\hbar}{2M\Omega(x_c)}\frac{1+2\sinh^2(\Omega(x_c)(\beta\hbar/2-\tau))}{\sinh(\Omega(x_c)\beta\hbar)} \\ &\quad + {a_{FK}}^2(x_c) - \frac{\hbar}{2M\Omega(x_c)\sinh(\Omega(x_c)\beta\hbar)}\end{aligned} \tag{78}$$

or

https://doi.org/10.1021/acs.jpca.1c05860
J. Phys. Chem. A 2021, 125, 9209−9225

$$\langle x^2(\tau)\rangle_{tr} = x_c^2 + a_{FK}^2(x_c) + \frac{\hbar}{M\Omega(x_c)}\frac{\sinh^2(\Omega(x_c)(\beta\hbar/2-\tau))}{\sinh(\Omega(x_c)\beta\hbar)} \quad (79)$$

which is eq 35.

APPENDIX B

Path Integral Using Open Path Fourier Modes

Here we show how to write the path integral representation of the Boltzmann operator using Fourier modes. Normally, this is done assuming closed paths, using the so-called Matsubara frequency representation.[19] Here, we do it for open paths, which to our knowledge is much less explored. As an example, we consider the calculation of the off-diagonal trace $\Delta = \int dx_c\, \Delta(x_c)$ for a one-dimensional particle with mass M moving in a potential $V(x)$ at an inverse temperature $\beta = 1/k_BT$. In Cartesian coordinates, using N beads, we have

$$\Delta = \int_{-\infty}^{\infty} dx \int_{-\infty}^{\infty} dy\, \langle x|\exp(-\beta\hat{H})|y\rangle = \int_{-\infty}^{\infty} dx_1 \ldots \int_{-\infty}^{\infty} dx_N \prod_{k=1}^{N-1} \langle x_k|\exp\left(-\frac{\beta}{N-1}\hat{H}\right)|x_{k+1}\rangle \quad (80)$$

Using the high temperature approximation (writing $\beta' = \beta/(N-1)$)

$$\begin{aligned}\langle x_k|\exp(-\beta'\hat{H})|x_{k+1}\rangle &\approx \frac{1}{2\pi\hbar}\int_{-\infty}^{\infty} dp\, \exp\left(-\beta'\left[\frac{p^2}{2M} + \frac{V(x_k)+V(x_{k+1})}{2}\right] - \frac{i}{\hbar}p(x_{k+1}-x_k)\right)\\ &= \left(\frac{M}{\beta' 2\pi\hbar^2}\right)^{1/2}\exp\left(-\frac{M}{2}\frac{1}{\beta'\hbar^2}(x_{k+1}-x_k)^2 - \beta'\frac{V(x_k)+V(x_{k+1})}{2}\right)\end{aligned} \quad (81)$$

we obtain

$$\begin{aligned}\Delta &= \left(\frac{M(N-1)}{\beta 2\pi\hbar^2}\right)^{(N-1)/2}\prod_{k=1}^{N}\int_{-\infty}^{\infty} dx_k \exp\left(-\frac{M}{2}\frac{N-1}{\beta\hbar^2}\sum_{k=1}^{N-1}(x_{k+1}-x_k)^2\right)\times\exp\left(-\frac{\beta}{N-1}\sum_{k=2}^{N-1}V(x_k) - \frac{\beta}{N-1}\frac{V(x_1)+V(x_N)}{2}\right)\\ &= \left(\frac{M(N-1)}{\beta 2\pi\hbar^2}\right)^{(N-1)/2}\int d\vec{x}_N \exp\left(-\frac{M}{2}\frac{N-1}{\beta\hbar^2}\sum_{k=1}^{N-1}(x_{k+1}-x_k)^2 - \frac{\beta}{N-1}V(\vec{x}_N)\right)\end{aligned} \quad (82)$$

where we have introduced some short-hand notation: $\vec{x}_N = (x_1, \ldots, x_N)$ and $V(\vec{x}_N) = \sum_{k=2}^{N-1}V(x_k) + \frac{V(x_1)+V(x_N)}{2}$. We next introduce the normal modes of the kinetic energy, which is written in the form $\sum_{k=1}^{N-1}(x_{k+1}-x_k)^2$.[29] The jth normal mode is

$$\nu_j = \sum_{k=1}^{N} Q_{jk}x_k, \qquad j = 0, \ldots, N-1 \quad (83)$$

where the orthonormal $N \times N$ matrix Q has components

$$Q_{jk} = \left(\frac{2-\delta_{j0}}{N}\right)^{1/2}\cos\left(\frac{\left(k-\frac{1}{2}\right)j\pi}{N}\right), \quad j = 0, \ldots, N-1,\ k = 1, \ldots, N \quad (84)$$

The eigenvalue of ν_j is

$$\lambda_j = 4\sin^2\left(\frac{j\pi}{2N}\right) \quad (85)$$

It follows that

$$x_k = \sum_{j=0}^{N-1} Q_{kj}^{T}\nu_j \quad (86)$$

By expressing eq 82 in terms of normal modes, it becomes

$$\Delta = \left(\frac{M(N-1)}{\beta 2\pi\hbar^2}\right)^{(N-1)/2}\int d\vec{\nu}_N \exp\left(-\frac{M}{2}\frac{N-1}{\beta\hbar^2}\times\sum_{j=0}^{N-1}4\sin^2\left(\frac{j\pi}{2N}\right)\nu_j^2 - \frac{\beta}{N-1}V(\vec{\nu}_N)\right) \quad (87)$$

We have written $\vec{\nu}_N = (\nu_0, \ldots, \nu_{N-1})$ and utilized that $\int d\vec{\nu}_N = \int d\vec{x}_N$ since the determinant of the Jacobian of the mapping between $\vec{\nu}_N$ and $\vec{x}_N$ is unity. For mathematical convenience we will define $\vec{\eta}_N = (1/N)^{1/2}\vec{\nu}_N$. It follows that η_0 is the centroid of the path. We can write

$$\Delta = \left(\frac{M(N-1)}{\beta 2\pi\hbar^2}\right)^{(N-1)/2}N^{N/2}\int d\vec{\eta}_N \exp\left(-\frac{M}{2}\frac{N\cdot(N-1)}{\beta\hbar^2}\times\sum_{j=0}^{N-1}4\sin^2\left(\frac{j\pi}{2N}\right)\eta_j^2 - \frac{\beta}{N-1}V(\vec{\eta}_N)\right) \quad (88)$$

One final coordinate transformation is needed. We set

$$a_j = 2^{1/2}\frac{2\sin\left(\frac{j\pi}{2N}\right)}{j\pi}(N\cdot(N-1))^{1/2}\cdot\eta_j, \quad j = 1, \ldots, N-1 \quad (89)$$

and

$$a_0 = \eta_0 \quad (90)$$

Again we write $\vec{a}_N = (a_0,..,a_{N-1})$. Equation 88 tranforms into

$$\Delta = \left(\frac{M(N-1)}{\beta 4\pi\hbar^2}\right)^{(N-1)/2}N^{N/2}(N\cdot(N-1))^{-(N-1)/2}\prod_{j=1}^{N-1}\frac{j\pi}{2\sin\left(\frac{j\pi}{2N}\right)}\times\int d\vec{a}_N \exp\left(-\frac{M}{4}\beta\sum_{j=0}^{N-1}\left(\frac{j\pi}{\beta\hbar}\right)^2 a_j^2 - \frac{\beta}{N-1}V(\vec{a}_N)\right) \quad (91)$$

Using the identity (see proof at the end of this section)

https://doi.org/10.1021/acs.jpca.1c05860
J. Phys. Chem. A 2021, 125, 9209−9225

$$\prod_{j=1}^{N-1} \frac{1}{2\sin\left(\frac{j\pi}{2N}\right)} = N^{-1/2} \tag{92}$$

Equation 91 can be simplified to

$$\begin{aligned}\Delta &= \left(\frac{M}{\beta 4\pi\hbar^2}\right)^{(N-1)/2} \prod_{j=1}^{N-1} j\pi \times \int d\vec{a}_N \exp\left(-\frac{M}{4}\beta \sum_{j=0}^{N-1}\left(\frac{j\pi}{\beta\hbar}\right)^2 {a_j}^2 \right.\\ &\quad \left. - \frac{\beta}{N-1} V(\vec{a}_N)\right)\\ &= \int da_0 \prod_{j=1}^{N-1} \int da_j \left(\frac{{\omega_j}^2 \beta M}{4\pi}\right)^{1/2} \exp\left(-\frac{M}{4}\beta \sum_{j=0}^{N-1} {\omega_j}^2 {a_j}^2 \right.\\ &\quad \left. - \frac{\beta}{N-1} V(\vec{a}_N)\right)\end{aligned} \tag{93}$$

where $\omega_j = \frac{j\pi}{\beta\hbar}$, $j = 0, ..., N-1$. Equation 93 is the Fourier representation of the path integral.

We next consider the equation for a_j ($j \neq 0$):

$$\begin{aligned}a_j &= 2^{1/2} \frac{2\sin\left(\frac{j\pi}{2N}\right)}{j\pi} (N\cdot(N-1))^{1/2} \cdot\\ &\quad N^{-1/2}\left(\frac{2}{N}\right)^{1/2} \sum_{k=1}^{N} \cos\left(\frac{\left(k-\frac{1}{2}\right)j\pi}{N}\right) x_k\end{aligned} \tag{94}$$

Fix a value of j. If N is large in eq 94, this expression may be written (use $\sin(x)/x \to 1$, $x \to 0$)

$$\begin{aligned}a_j &= 2\frac{1}{\beta\hbar}\sum_{k=1}^{N} \frac{\beta\hbar}{N} \cos\left(\frac{\left(k-\frac{1}{2}\right)j\pi}{N}\right) x_k\\ &= 2\frac{1}{\beta\hbar}\sum_{k=1}^{N} \frac{\beta\hbar}{N} \cos\left(\frac{\frac{k-\frac{1}{2}}{N}\beta\hbar j\pi}{\beta\hbar}\right) x_k\\ &= 2\frac{1}{\beta\hbar}\sum_{k=1}^{N} \frac{\beta\hbar}{N} \cos\left(\frac{\tau_k \cdot j\pi}{\beta\hbar}\right) x_k \to 2\frac{1}{\beta\hbar}\int_0^{\beta\hbar} d\tau \cos(\tau\omega_j)\, x(\tau),\\ &\quad N \to \infty\end{aligned} \tag{95}$$

We have discretized the time axis as $\tau_k = \frac{k-\frac{1}{2}}{N}\beta\hbar$, $k = 1, ..., N$. For $j = 0$, we obtain similarly

$$\begin{aligned}a_0 &= \frac{1}{N}\sum_{k=1}^{N} x_k = \frac{1}{\beta\hbar}\sum_{k=1}^{N} \frac{\beta\hbar}{N} \cos\left(\frac{\tau_k \cdot 0\cdot\pi}{\beta\hbar}\right) x_k\\ &\to \frac{1}{\beta\hbar}\int_0^{\beta\hbar} d\tau \cos(\tau\omega_0) x(\tau), \qquad N \to \infty\end{aligned} \tag{96}$$

We recognize eqs 95 and 96 as eq 31 and eq 30, respectively. Thus, we have rederived the Fourier representation of $x(\tau)$.

We may also consider the expression for x_k in terms of the normal modes in the limit $N \to \infty$. Again, let $\tau_k = \frac{k-\frac{1}{2}}{N}\beta\hbar$, $k = 1, ..., N$. From eq 86 we get

$$\begin{aligned}x_k = x(\tau_k) &= \sum_{j=0}^{N-1} Q_{kj}^{\mathrm{T}} \nu_j\\ &= \sum_{j=0}^{N-1} \left(\frac{2}{N}\right)^{1/2} \cos\left(\frac{\left(k-\frac{1}{2}\right)j\pi}{N}\right) \nu_j\\ &= \sum_{j=0}^{N-1} \left(\frac{2}{N}\right)^{1/2} \cos\left(\frac{\left(k-\frac{1}{2}\right)j\pi}{N}\right) N^{1/2}\\ &\quad \times \frac{a_j}{2^{1/2}\frac{2\sin\left(\frac{j\pi}{2N}\right)}{j\pi}(N\cdot(N-1))^{1/2}}\end{aligned} \tag{97}$$

To proceed, we need to show that $\gamma(j, N) \equiv 2\sin\left(\frac{j\pi}{2N}\right)(N\cdot(N-1))^{1/2}/j\pi$ can be set equal to unity for large N. This is correct as long as $j \ll N$. At first sight, this is not possible since j runs all the way up to $N-1$. However, all realistic paths $x(\tau)$ that contribute to the path integral have a frequency cut-off $j \leq j_{max}$ which results from the kinetic energy part of the path integral. Therefore, if j is so big that $\gamma(j, N)$ is not unity, then j will by far exceed j_{max} if N is big enough. Thus, if $j > j_{max}$ then only $a_j = 0$ contributes to the path integral and it will not matter if we put $\gamma(j, N) = 1$ in eq 97.

If N becomes large in eq 97 and k likewise so that $\tau = \frac{k-\frac{1}{2}}{N}\beta\hbar$ is constant, then we get the following expression for $x(\tau_k)$:

$$\begin{aligned}x(\tau_k) &= \sum_{j=0}^{j_{max}} \cos\left(\frac{\left(k-\frac{1}{2}\right)j\pi}{N}\right) a_j\\ &= \sum_{j=0}^{j_{max}} \cos\left(\frac{j\pi}{\beta\hbar}\frac{\left(k-\frac{1}{2}\right)\beta\hbar}{N}\right) a_j\\ &\Rightarrow x(\tau) = \sum_{j=0}^{\infty} \cos(\omega_j\tau) a_j, \qquad N \to \infty\end{aligned} \tag{98}$$

This is eq 28.

We finally show how to express the potential energy part of the path integral in terms of Fourier modes as done in eq 93. The part is

$$\begin{aligned}\frac{\beta}{N-1} V(\vec{x}_N) &= \frac{\beta}{N-1}\left[\sum_{k=2}^{N-1} V(x_k) + \frac{V(x_1) + V(x_N)}{2}\right]\\ &\approx \frac{\beta}{N-1}\sum_{k=1}^{N} V(x_k)\end{aligned} \tag{99}$$

This rewriting should be acceptable for large N. When $N \to \infty$, this becomes

$$\begin{aligned}\frac{\beta}{N-1}\sum_{k=1}^{N} V(x_k) &\to \int_0^{\beta\hbar} d\tau\, V(x(\tau))/\hbar\\ &= \int_0^{\beta\hbar} d\tau\, V\Big(\sum_{j=0}^{\infty} \cos(\omega_j\tau) a_j\Big)/\hbar\end{aligned} \tag{100}$$

Then we may finally write the total path integral in eq 93 as

https://doi.org/10.1021/acs.jpca.1c05860
J. Phys. Chem. A 2021, 125, 9209−9225

$$\Delta = \int \mathrm{d}a_0 \prod_{j=1}^{\infty} \int \mathrm{d}a_j \left(\frac{\omega_j^2 \beta M}{4\pi}\right)^{1/2} \exp\left(-\frac{M}{4}\beta \sum_{j=0}^{\infty} \omega_j^2 a_j^2 - \int_0^{\beta\hbar} \mathrm{d}\tau\, V\left(\sum_{j=0}^{\infty} \cos(\omega_j \tau) a_j\right)/\hbar\right) \tag{101}$$

where we have taken the limit $N \to \infty$.

Equation 101 is the central result of this appendix. If we restrict the centroid a_0 to be $a_0 = x_c$ and consider a potential $V(x(\tau)) = L(x_c) + \frac{1}{2}M\Omega^2(x_c)(x(\tau) - x_c)^2$, then we may show that eq 101 rederives the result in eq 22.

We remember that eq 101 is the Boltzmann path integral over *all* open paths. If we want to calculate matrix elements such as, e.g., $\langle x|\exp(-\beta\hat{H})|y\rangle$ we can apply eq 101 if we add two extra integrations $\delta(y - x(0)) = \int \mathrm{d}\theta_1 \exp(\mathrm{i}\theta_1(y - x(0)))/2\pi = \int \mathrm{d}\theta_1 \exp(\mathrm{i}\theta_1(y - a_0 - a_1 - \ldots))/2\pi$ and $\delta(x - x(\beta\hbar)) = \int \mathrm{d}\theta_2 \exp(\mathrm{i}\theta_2(x - a_0 + a_1 - a_2 + \ldots))/2\pi$. In this Gaussian integral, we first integrate out all $(a_0, a_1, \ldots)$, followed by integrating out θ_1 and θ_2. In this way, also eq 75 can be derived by simply fixing the centroid a_0 to be $a_0 = x_c$.

Let us finally return to the identity in eq 92. To prove it, we start with the result 1.392.1 in ref 30

$$\sin nx = 2^{n-1} \prod_{k=0}^{n-1} \sin\left(x + \frac{k\pi}{n}\right) \tag{102}$$

Letting $x \to 0$, we obtain

$$n = 2^{n-1} \prod_{k=1}^{n-1} \sin\left(\frac{k\pi}{n}\right) \tag{103}$$

Next, let $n = 2m$ be even. Observe that the arguments of the sine functions go through half the unit circle, symmetrically around $\pi/2$. By using $\sin\left(\frac{k\pi}{n}\right) = \sin\left(\frac{(n-k)\pi}{n}\right)$, we may limit the sine arguments to the first quarter of the unit circle only, instead squaring the result. Thus

$$2m = \prod_{k=1}^{2m-1} 2\sin\left(\frac{k\pi}{2m}\right) \Leftrightarrow 2m = 2\left(\prod_{k=1}^{m-1} 2\sin\left(\frac{k\pi}{2m}\right)\right)^2 \tag{104}$$

or

$$m^{1/2} = \prod_{k=1}^{m-1} 2\sin\left(\frac{k\pi}{2m}\right) \tag{105}$$

which was to be proved.

■ ASSOCIATED CONTENT

Supporting Information

The Supporting Information is available free of charge at https://pubs.acs.org/doi/10.1021/acs.jpca.1c05860.

Calculation of matrix elements of the Boltzmann operator using Fourier Modes - the harmonic oscillator case (PDF)

■ AUTHOR INFORMATION

Corresponding Author

Gunnar Nyman − *Department of Chemistry and Molecular Biology, University of Gothenburg, SE 405 30 Gothenburg, Sweden;* orcid.org/0000-0002-9527-3890; Email: gunnar.nyman@gu.se

Author

Jens Aage Poulsen − *Department of Chemistry and Molecular Biology, University of Gothenburg, SE 405 30 Gothenburg, Sweden;* orcid.org/0000-0002-6675-8485

Complete contact information is available at: https://pubs.acs.org/10.1021/acs.jpca.1c05860

Notes

The authors declare no competing financial interest.

■ ACKNOWLEDGMENTS

This work has been supported by the Swedish Research Council through grant 2020-05293.

■ ADDITIONAL NOTES

[a]We notice that by adopting the standard N-bead time-sliced path integral approximation to $\Delta(x_c)$, we obtain the classical partition function for an N-bead polymer which is held together by harmonic springs with force constants $k = M(N-1)^2/(\beta\hbar)^2$ and moves in the external potential $V(x)$ at inverse temperature $\beta/(N-1)$. Its center of mass is fixed at x_c. See Appendix B for the details of this derivation.

[b]When evaluating eq 33, the determinant of the Jacobian which is associated with the mapping from Cartesian coordinates to Fourier modes is not needed, since we are calculating the ratio of two path integrals.

■ REFERENCES

(1) Wigner, E. On the Quantum Correction For Thermodynamic Equilibrium. *Phys. Rev.* **1932**, *40*, 749.

(2) Zachos, C. K., Fairlie, D. B., Curtright, T. L., Eds. *Quantum Mechanics in Phase Space*; World Scientific, 2005.

(3) Poulsen, J. A.; Nyman, G.; Rossky, P. J. Practical evaluation of condensed phase quantum correlation functions: A Feynman−Kleinert variational linearized path integral method. *J. Chem. Phys.* **2003**, *119*, 12179−12193.

(4) Wang, H.; Sun, X.; Miller, W. H. Semiclassical approximations for the calculation of thermal rate constants for chemical reactions in complex molecular systems. *J. Chem. Phys.* **1998**, *108*, 9726−9736.

(5) Shi, Q.; Geva, E. Semiclassical Theory of Vibrational Energy Relaxation in the Condensed Phase. *J. Phys. Chem. A* **2003**, *107*, 9059−9069.

(6) Bose, A.; Makri, N. Wigner Distribution by Adiabatic Switching in Normal Mode or Cartesian Coordinates and Molecular Applications. *J. Chem. Theory Comput.* **2018**, *14*, 5446−5458.

(7) Plé, T.; Huppert, S.; Finocchi, F.; Depondt, P.; Bonella, S. Sampling the thermal Wigner density via a generalized Langevin dynamics. *J. Chem. Phys.* **2019**, *151*, 114114.

(8) Marinica, D. C.; Gaigeot, M.-P.; Borgis, D. Generating approximate Wigner distributions using Gaussian phase packets propagation in imaginary time. *Chem. Phys. Lett.* **2006**, *423*, 390−394.

(9) Smith, K. K. G.; Poulsen, J.; Nyman, G.; Rossky, P. J. A new class of ensemble conserving algorithms for approximate quantum dynamics: Theoretical formulation and model problems. *J. Chem. Phys.* **2015**, *142*, 244112.

(10) Svensson, K.-M.; Poulsen, J.; Nyman, G. Classical Wigner model based on a Feynman path integral open polymer. *J. Chem. Phys.* **2020**, *152*, 094111.

(11) Weinbub, J.; Ferry, D. K. Recent advances in Wigner function approaches. *Appl. Phys. Rev.* **2018**, *5*, 041104.

(12) Liu, J.; Miller, W. H. A simple model for the treatment of imaginary frequencies in chemical reaction rates and molecular liquids. *J. Chem. Phys.* **2009**, *131*, 074113.

(13) Liu, J.; Miller, W. H. Using the thermal Gaussian approximation for the Boltzmann operator in semiclassical initial value time correlation functions. *J. Chem. Phys.* **2006**, *125*, 224104.
(14) Liu, J.; Miller, W. H. An approach for generating trajectory-based dynamics which conserves the canonical distribution in the phase space formulation of quantum mechanics. II. Thermal correlation functions. *J. Chem. Phys.* **2011**, *134*, 104102.
(15) Poulsen, J. A.; Nyman, G.; Rossky, P. J. Feynman-Kleinert Linearized Path Integral (FK-LPI) Algorithms for Quantum Molecular Dynamics, with Application to Water and He(4). *J. Chem. Theory Comput.* **2006**, *2*, 1482−1491.
(16) Liu, J. Recent advances in the linearized semiclassical initial value representation/classical Wigner model for the thermal correlation function. *Int. J. Quantum Chem.* **2015**, *115*, 657−670.
(17) Poulsen, J. A.; Nyman, G.; Rossky, P. J. Static and dynamic quantum effects in molecular liquids: A linearized path integral description of water. *Proc. Natl. Acad. Sci. U. S. A.* **2005**, *102*, 6709−6714.
(18) Feynman, R. P.; Kleinert, H. Effective classical partition functions. *Phys. Rev. A: At., Mol., Opt. Phys.* **1986**, *34*, 5080−5084.
(19) Kleinert, H. *Path Integrals in Quantum Mechanics, Statistics, Polymer Physics, and Financial Markets*, 5th ed.; World Scientific: Singapore, 2009.
(20) Poulsen, J. A.; Nyman, G.; Rossky, P. J. Determination of the Van Hove Spectrum of liquid He(4): An application of the Feynman-Kleinert Linearized Path Integral Methodology. *J. Phys. Chem. A* **2004**, *108*, 8743−8751.
(21) Scheers, J.; Poulsen, J. A.; Nyman, G.; Rossky, P. J. Quantum density fluctuations in liquid neon from linearized path-integral calculations. *Phys. Rev. B: Condens. Matter Mater. Phys.* **2007**, *75*, 224505.
(22) Smith, K. K. G.; Poulsen, J.; Nyman, G.; Cunsolo, A.; Rossky, P. J. Application of a new ensemble conserving quantum dynamics simulation algorithm to liquid para-hydrogen and ortho-deuterium. *J. Chem. Phys.* **2015**, *142*, 244113.
(23) Poulsen, J. A.; Nyman, G.; Rossky, P. J. Quantum Diffusion in Liquid Para-hydrogen: An Application of the Feynman-Kleinert Linearized Path Integral Approximation. *J. Phys. Chem. B* **2004**, *108*, 19799−19808.
(24) Hone, T. D.; Poulsen, J. A.; Rossky, P. J.; Manolopoulos, D. E. Comparison of Approximate Quantum Simulation Methods Applied to Normal Liquid Helium at 4 K. *J. Phys. Chem. B* **2008**, *112*, 294−300.
(25) Cover, T. M.; Joy, T. A. *Elements of Information Theory*, 2nd ed.; Wiley-Interscience, 2006.
(26) Taylor, A. E. Differentiation of Fourier Series and Integrals. *American Mathematical Monthly* **1944**, *51*, 19−25.
(27) Feynman, R. P. *Statistical Mechanics: A set of Lectures*; Addison-Wesley: Boston, MA, 1998.
(28) Poulsen, J.; Huaqing, L.; Nyman, G. Classical Wigner method with an effective quantum force: Application to reaction rates. *J. Chem. Phys.* **2009**, *131*, 024117.
(29) Verdier, P. H. Monte Carlo Studies of Lattice-Model Polymer Chains. I. Correlation Functions in the Statistical-Bead Model. *J. Chem. Phys.* **1966**, *45*, 2118−2121.
(30) Gradshteyn, I. S., Ryzhik, I. M., Eds. *Table of Integrals, Series, and Product*, 7th ed.; Elsevier/Academic Press: Amsterdam, 2007.

https://doi.org/10.1021/acs.jpca.1c05860
J. Phys. Chem. A 2021, 125, 9209−9225